

Quark-Lepton Connections in Z' Mediated FCNC Processes: Gauge Anomaly Cancellations at Work

Jason Aebischer^a, Andrzej J. Buras^b,
Maria Cerdà-Sevilla^c and Fulvia De Fazio^d

^a Department of Physics, University of California at San Diego, La Jolla, CA 92093, USA

^bTUM Institute for Advanced Study, Lichtenbergstr. 2a, D-85747 Garching, Germany

^c Excellence Cluster Universe, Boltzmannstr. 2, 85748 Garching, Germany

^dIstituto Nazionale di Fisica Nucleare, Sezione di Bari, Via Orabona 4, I-70126 Bari, Italy

Abstract

We consider scenarios with a heavy Z' gauge boson with flavour non-universal quark and lepton couplings with the goal to illustrate how the cancellation of gauge anomalies generated by the presence of an additional $U(1)'$ gauge symmetry would imply correlations between FCNC processes within the quark sector, within the lepton sector and most interestingly between quark flavour and lepton flavour violating processes. To this end we present simple scenarios with only left-handed flavour-violating Z' couplings and those in which also right-handed flavour-violating couplings are present. The considered scenarios are characterized by a small number of free parameters but in contrast to gauge anomaly cancellation in the Standard Model, in which it takes place separately within each generation, in our scenarios anomaly cancellation involves simultaneously quarks and leptons of all three generations. Our models involve, beyond the ordinary quarks and leptons, three heavy right-handed neutrinos. The models with only left-handed FCNCs of Z' involve beyond $g_{Z'}$ and $M_{Z'}$ two real parameters characterizing the charges of all fermions under the $U(1)'$ gauge symmetry and the CKM and PMNS ones in the quark and lepton sectors, respectively. The models with the right-handed FCNCs of Z' involve few additional parameters. Imposing constraints from well measured $\Delta F = 2$ observables we identify a number of interesting correlations that involve e.g. ε'/ε , $B_{s,d} \rightarrow \mu^+\mu^-$, $B \rightarrow K(K^*)\ell^+\ell^-$, $K^+ \rightarrow \pi^+\nu\bar{\nu}$, $K_L \rightarrow \pi^0\nu\bar{\nu}$ and purely lepton flavour violating decays like $\mu \rightarrow e\gamma$, $\mu \rightarrow 3e$, $\tau \rightarrow 3\mu$ and $\mu - e$ conversion among others. Also $(g-2)_{\mu,e}$ are considered. The impact of the experimental $\mu \rightarrow e\gamma$, $\mu \rightarrow 3e$ and in particular $\mu - e$ conversion bounds on rare K and B decays is emphasized.

Contents

1	Introduction	2
2	Basic Gauge Anomaly Equations	3
2.1	Basic Lagrangian for Z'	3
2.2	General Formulae	4
2.3	Solution to linear equations	5
2.4	Example 1	5
2.5	Example 2	6
3	A simple model for gauge anomaly cancellation	6
3.1	Cancellation of gauge anomalies	6
3.2	Rotation of fermions to the mass eigenstate basis	8
3.2.1	General formulation	8
3.2.2	Rotation to mass eigenstates: quarks	8
3.2.3	Rotation to mass eigenstates: leptons	11
4	Considered observables	13
4.1	Preliminaries	13
4.2	$\mu \rightarrow e\gamma$, $\tau \rightarrow \mu\gamma$ and $\tau \rightarrow e\gamma$	13
4.3	Three-body Lepton decays	13
4.4	$\mu - e$ conversion in nuclei	14
4.5	$(g - 2)_\mu$ and $(g - 2)_e$	15
5	Various coupling scenarios	15
5.1	Preliminaries and general strategy for numerics	15
5.2	Different Scenarios	16
5.2.1	Scenario A	16
5.2.2	Scenarios B1 and B2	17
5.2.3	Scenario C	18
6	Numerical Analysis	18
6.1	Results in Scenario A	18
6.2	Results in Scenario B1	20
6.3	Results in Scenario B2	23
6.4	Results in Scenario C	24
7	Conclusions	30
A	Removing $\Delta F = 2$ Constraints	32

1 Introduction

Among the simplest new physics (NP) scenarios there are the ones with a new heavy neutral gauge boson Z' and the associated gauge symmetry $U(1)'$. There is a long history of Z' models with selected papers and reviews given in [1–3]. In particular, already long time ago Z' models with flavour-non-universal couplings to SM fermions have been considered [4–8]. In the context of recently very popular B -physics anomalies selected papers are given in [9, 10].

One of the important issues in such models is the cancellation of the gauge anomalies that naturally are generated in the presence of an additional $U(1)'$ gauge group. This case has been studied in [9, 11–18] in the context of collider processes and B -physics anomalies but in most of these papers, the exception being [9, 12], flavour universality either in the lepton sector or quark sector or in both has been assumed. But even in [12] Z' couplings to the first generation of quarks have been set to zero in order to avoid stringent constraints from the Kaon sector and in most papers new complex phases have been set to zero as they were not required to explain B -physics anomalies.

On the other hand, Kaon physics has still a lot to offer. In particular the ratio ε'/ε [19], that describes the amount of direct CP violation in $K_L \rightarrow \pi\pi$ decays relative to the indirect one, still allows for significant NP contributions and this also applies to rare Kaon decays $K^+ \rightarrow \pi^+\nu\bar{\nu}$ and $K_L \rightarrow \pi^0\nu\bar{\nu}$.

But in addition to FCNC processes in the quark sector, an increasing role in the coming years will be played by purely leptonic processes like $\mu \rightarrow e\gamma$, $\mu \rightarrow 3e$, $\tau \rightarrow 3\mu$ and $\mu - e$ conversion among others. Also $(g - 2)_{\mu,e}$ is of great interest in view of the hints for NP and the new measurement of $(g - 2)_\mu$ expected soon from Fermilab.

Recently, some correlations between B -physics anomalies and in particular τ decays through renormalization group effects have been pointed out in various papers but mostly in the context of leptoquark models or in the context of SMEFT analyses of these anomalies. Selected papers can be found in [20–23].

In the present paper we want to look simultaneously at most important FCNC processes in the quark and lepton sectors in the context of scenarios with a heavy Z' gauge boson with flavour non-universal quark and lepton couplings with the goal to illustrate how the correlations between various observables are implied not through SMEFT RG effects or flavour symmetries but through the cancellation of gauge anomalies generated through the presence of an additional $U(1)'$ gauge symmetry.

In general Z' models, like those considered in [1–3], it is assumed that gauge anomalies in question are canceled by some very heavy fermions whose contributions to rare decays are strongly suppressed. Without some flavour symmetries the flavour violating Z' couplings in different meson systems and in charged lepton decays are then independent of each other and this also applies to flavour conserving couplings. However, if the cancellation of gauge anomalies should take place without new particles beyond the ordinary quarks and leptons, these couplings cannot be arbitrary. This, as we will demonstrate in our paper, implies correlations between FCNC processes within the quark sector, within the lepton sector and most interestingly between quark flavour and lepton flavour violating processes. To this end we present simple scenarios with only left-handed (LH) flavour-violating Z' couplings and those in which also right-handed (RH) flavour-violating couplings are present. The considered scenarios are characterized by a small number of free parameters but in contrast to gauge anomaly cancellation in the Standard Model (SM), in which it takes place separately within each generation, in our scenarios

anomaly cancellation involves simultaneously quarks and leptons of all three generations.

The considered model involves, besides the SM quarks and leptons, three heavy RH neutrinos. Furthermore a heavy scalar, assumed to be a singlet under the SM gauge symmetry, is needed to provide a mass to the Z' . Scenarios with only LH FCNCs generated by the Z' involve besides $g_{Z'}$ and $M_{Z'}$ two real parameters characterizing the $U(1)'$ charges of all fermions. Further parameters stem from the CKM- and PMNS-like matrices in the quark and lepton sector, respectively. Scenarios with the RH FCNC Z' -couplings involve few additional parameters. Imposing constraints from precisely measured $\Delta F = 2$ observables we identify a number of interesting correlations that involve the B -decays $B_{s,d} \rightarrow \mu^+ \mu^-$, $B \rightarrow K(K^*) \ell^+ \ell^-$, the Kaon observables ε'/ε , $K^+ \rightarrow \pi^+ \nu \bar{\nu}$, $K_L \rightarrow \pi^0 \nu \bar{\nu}$ and purely lepton flavour violating decays like $\mu \rightarrow e \gamma$, $\mu \rightarrow 3e$, $\tau \rightarrow 3\mu$ and $\mu - e$ conversion among others. Furthermore $(g - 2)_{\mu,e}$ are considered.

The outline of our paper is as follows. In Section 2 we define the Z' couplings to SM particles that are characterized by their charges under the $U(1)'$ gauge symmetry and we list all equations that these charges have to satisfy to ensure the absence of gauge anomalies. In Section 3 we present a simple model for gauge anomaly cancellation that involves only a few new parameters. In Section 4 we list the observables considered by us together with the references to our previous papers where the relevant formulae in the same notation can be found. For charged lepton decays, $\mu - e$ conversion and $(g - 2)_{\mu,e}$ we give explicit formulae because they cannot be found there.

In Section 5 we present different scenarios for the couplings distinguishing between models with and without RH flavour violating couplings. The numerical analysis of these scenarios is presented in Section 6. Finally, we summarize in Section 7.

2 Basic Gauge Anomaly Equations

2.1 Basic Lagrangian for Z'

We start with the basic Lagrangian describing the interactions of the Z' gauge boson with SM fermions in the flavour basis. Generally, $Z - Z'$ mixing is present, but we will neglect it in the present paper as it does not affect the points we want to make. Thus, Z' in our paper is from the beginning in the mass-eigenstate basis.

Using the notation of [3], we have then

$$\mathcal{L}(Z') = \sum_{i,j,\psi_L} \Delta_L^{ij}(Z') \bar{\psi}_L^i \gamma^\mu P_L \psi_L^j Z'_\mu + \sum_{i,j,\psi_R} \Delta_R^{ij}(Z') \bar{\psi}_R^i \gamma^\mu P_R \psi_R^j Z'_\mu, \quad (1)$$

where $P_{L,R} = (1 \mp \gamma_5)/2$. Here ψ represent classes of fermions with the same electric charge, i.e., u, d, e, ν , while i, j are generation indices: 1, 2, 3. For instance $u_3 = t$ and $e_2 = \mu$. The couplings $\Delta_{L,R}^{ij}(Z')$ are given as follows

$$\Delta_L^{ij}(Z') = g_{Z'} z_{\psi_L^i} \delta^{ij}, \quad \Delta_R^{ij}(Z') = g_{Z'} z_{\psi_R^i} \delta^{ij}, \quad (2)$$

with $z_{\psi_L^i}$ and $z_{\psi_R^i}$ being fermion charges under $U(1)'$.

It should be noted that Z' couplings are flavour conserving at this stage, but the charges $z_{\psi_L^i}$ and $z_{\psi_R^i}$ will generally depend on the generation index i . This is necessary in order to generate FCNCs mediated by the Z' through the rotation of fermions to the mass eigenstate basis. We will perform this rotation in Section 3.2, but as the cancellation

of anomalies can be performed in the flavour basis, we continue our discussion in this basis.

In the present paper we will consider only scenarios with SM fermions, except possibly RH neutrinos. We leave for the future the analysis of scenarios with additional fermions which are vectorial with respect to the SM gauge group but not with respect to $U(1)'$ so that possible left-over gauge anomalies can be cancelled by these new fermions.

As the Z' is a singlet under the SM gauge group, the LH leptons in a given doublet ℓ_i with $i = 1, 2, 3$ must have the same $U(1)'$ charges and similar for the members of LH quark doublets q_i . On the other hand, the RH leptons ν_i and e_i can have different $U(1)'$ charges and the same for the RH quarks u_i and d_i . We will allow all these charges to be generation dependent. The RH neutrinos will sometimes turn out to be relevant for the cancellation of the gauge anomalies.

Denoting by q_i and ℓ_i LH doublets and by u_i , d_i , ν_i and e_i RH singlets allows us to drop the subscripts L and R on the fields that were present in the general formula (1).

Concerning the normalization of the hypercharge Y , we use

$$Q = T_3 + Y, \quad (3)$$

so that for SM fermions we have independently of the generation index i

$$y_{q_i} = 1/6, \quad y_{u_i} = 2/3, \quad y_{d_i} = -1/3, \quad y_{\ell_i} = -1/2, \quad y_{e_i} = -1. \quad (4)$$

2.2 General Formulae

There are six gauge anomalies generated by the presence of a Z' [11]. Four of them are linear in $U(1)'$ charges, one is quadratic and one cubic. It is useful to begin with the first four equations as they are simpler and teach us already something.

The structure of the four linear equations can be simplified by defining

$$z_q = z_{q_1} + z_{q_2} + z_{q_3}, \quad z_u = z_{u_1} + z_{u_2} + z_{u_3}, \quad z_d = z_{d_1} + z_{d_2} + z_{d_3}, \quad (5)$$

$$z_l = z_{l_1} + z_{l_2} + z_{l_3}, \quad z_\nu = z_{\nu_1} + z_{\nu_2} + z_{\nu_3}, \quad z_e = z_{e_1} + z_{e_2} + z_{e_3}. \quad (6)$$

The $[SU(3)_C]^2U(1)'$, $[SU(2)]^2U(1)'$ and $[U(1)_Y]^2U(1)'$ anomaly cancellation conditions can then be written respectively as

$$A_{33z} = 2z_q - z_u - z_d = 0, \quad (7)$$

$$A_{22z} = 3z_q + z_l = 0, \quad (8)$$

$$A_{11z} = \frac{1}{6}z_q - \frac{4}{3}z_u - \frac{1}{3}z_d + \frac{1}{2}z_l - z_e = 0. \quad (9)$$

The fourth linear condition involves two gravitons and a Z' and is given by

$$A_{GGz} = 3[2z_q - z_u - z_d] + 2z_l - z_e - z_\nu = 0, \quad (10)$$

but using (7) it reduces to

$$A_{GGz} = 2z_l - z_e - z_\nu = 0. \quad (11)$$

In order to write the remaining two anomaly cancellation conditions in a transparent form we define

$$z_f^{(3)} = \sum_{i=1,2,3} z_{f_i}^3, \quad z_f^{(2)} = \sum_{i=1,2,3} z_{f_i}^2. \quad (12)$$

In terms of this notation, the $U(1)_Y[U(1)']^2$ anomaly cancellation condition is given by

$$A_{1zz} = [z_q^{(2)} - 2z_u^{(2)} + z_d^{(2)}] - [z_l^{(2)} - z_e^{(2)}] = 0, \quad (13)$$

and the one for the $[U(1)']^3$ anomaly by

$$A_{zzz} = 3[2z_q^{(3)} - z_u^{(3)} - z_d^{(3)}] + [2z_l^{(3)} - z_\nu^{(3)} - z_e^{(3)}] = 0. \quad (14)$$

2.3 Solution to linear equations

There are four linear equations with six unknowns. This implies that we can express four of the charges in (5) and (6) in terms of remaining ones. We consider two cases.

d-case:

We choose as free parameters z_q and z_d , then

$$z_u = 2z_q - z_d, \quad z_l = -3z_q, \quad z_e = z_d - 4z_q, \quad z_\nu = -2z_q - z_d. \quad (15)$$

u-case:

We choose as free parameters z_q and z_u , then

$$z_d = 2z_q - z_u, \quad z_l = -3z_q, \quad z_e = -z_u - 2z_q, \quad z_\nu = -4z_q + z_u. \quad (16)$$

We emphasize that the simple relations (15) and (16) are model-independent. Moreover, it turns out that the solutions in the d - and u -case also solve, in the case of flavour universality, the quadratic and cubic equations (13)-(14). Furthermore the SM case for the hypercharges can be retrieved from the above relations. This is not surprising, since the same equations as (7), (8), (11) and (14) are obtained in the case of the $U(1)_Y$ gauge boson, by simply replacing $z_f \rightarrow y_f$. Indeed, the anomaly equations are solved by choosing $z_{q_i} = 1/6$ independently of i , as well as $z_{d_i} = -1/3$ in the d -case and $z_{u_i} = 2/3$ in the u -case.

In what follows we will present two simple examples for the $U(1)'$ charges that satisfy all gauge anomaly cancellation conditions. Afterwards we introduce the model on which our study is based.

2.4 Example 1

This example involves two parameters

$$a \equiv z_{q_1}, \quad \text{and} \quad b \equiv z_{d_1}, \quad (17)$$

and assumes the universality of $U(1)'$ charges of the remaining fermions of a given electric charge as well as vanishing $U(1)'$ charges of RH neutrinos. The cancellation of all gauge-anomalies implies then

$$z_{q_2} = z_{q_3} = -\frac{b}{2}, \quad z_{u_1} = 2a - b, \quad z_{u_2} = z_{u_3} = a - \frac{3}{2}b, \quad z_{d_2} = z_{d_3} = \frac{b}{2} - a, \quad (18)$$

$$z_{l_1} = z_{l_2} = z_{l_3} = b - a, \quad z_{e_1} = z_{e_2} = z_{e_3} = 2(b - a), \quad z_{\nu_1} = z_{\nu_2} = z_{\nu_3} = 0. \quad (19)$$

The virtue of this solution is the absence of any new particles. But the complete flavour universality in the lepton sector and the equality of charges in the second and third quark generation is its disadvantage. In particular, the B -physics anomalies cannot be addressed. This solution can then only be vital if the NP effects would dominantly be found in the K meson system. We hope this will not be the case and consequently we will not analyze phenomenological consequences of this solution below.

2.5 Example 2

Also this example involves two parameters

$$a \equiv z_{q_1}, \quad \text{and} \quad b \equiv z_{u_1}, \quad (20)$$

and assumes the universality of $U(1)'$ charges of the remaining fermions of a given electric charge as well as vanishing $U(1)'$ charges of RH neutrinos. The cancellation of all gauge-anomalies implies then

$$z_{q_2} = z_{q_3} = -a + \frac{b}{2}, \quad z_{u_2} = z_{u_3} = -2a + \frac{3}{2}b, \quad z_{d_1} = 2a - b, \quad z_{d_2} = z_{d_3} = -\frac{b}{2}, \quad (21)$$

$$z_{l_1} = z_{l_2} = z_{l_3} = a - b, \quad z_{e_1} = z_{e_2} = z_{e_3} = 2(a - b), \quad z_{\nu_1} = z_{\nu_2} = z_{\nu_3} = 0. \quad (22)$$

The criticism to the Solution 1 applies also here and we will not consider it any further, but these two examples demonstrate transparently that gauge anomaly cancellation implies correlations between the $U(1)'$ charges of quarks and leptons.

3 A simple model for gauge anomaly cancellation

3.1 Cancellation of gauge anomalies

In order to obtain phenomenologically more interesting scenarios we break flavour universality in all three families. But in order not to end up with many free parameters we break the flavour universality in a rather special manner.

To this end let us denote by f one of the following fermions: $f = q, u, d, \ell, e, \nu$ and let us add a generation index: f_i for $i = 1, 2, 3$. We know that the SM hypercharge is generation universal so that $y_{f_i} = y_f \forall i = 1, 2, 3$. We write the z -charge as:

$$z_{f_i} = y_f + \epsilon_i \quad (23)$$

so that we have

$$z_f = \sum_{i=1}^3 z_{f_i} = \sum_{i=1}^3 (y_f + \epsilon_i) = 3y_f + \sum_{i=1}^3 \epsilon_i = 3y_f + \epsilon, \quad \epsilon = \sum_{i=1}^3 \epsilon_i. \quad (24)$$

It should be noted that the breakdown of flavour universality has been made in a very special manner. Indeed, the parameters ϵ_i while generation dependent, are universal within a given generation. For instance ϵ_1 is the same not only for the members of the LH doublets q_1, ℓ_1 but also for RH singlets u_1, d_1, ν_1 and e_1 . This implies that the shifts ϵ_i

are vector-like which allows for a straightforward solution of all anomaly equations. But as hypercharges of LH and RH fields, as seen in (4), differ from each other the flavour conserving Z' couplings are not vector-like.

Let us first check that the linear anomaly equations are satisfied keeping in mind that they are satisfied when $z_{f_i} = y_{f_i} = y_f$.

- $A_{33z} = 2z_q - z_u - z_d = 0$.

Substituting z_f from (24) we find

$$A_{33z} = 2(3y_q + \epsilon) - (3y_u + \epsilon) - (3y_d + \epsilon) = 3(2y_q - y_u - y_d) = 0, \quad (25)$$

where the last equation holds since the hypercharges solve the anomaly equations.

- $A_{22z} = 3z_q + z_\ell = 0$.

We have

$$A_{22z} = 3(3y_q + \epsilon) + (3y_\ell + \epsilon) = 3(3y_q + y_\ell) + 4\epsilon = 4\epsilon, \quad (26)$$

where $(3y_q + y_\ell) = 0$ again because hypercharges solve the anomaly equations so that this equation is satisfied provided that $\epsilon = 0$.

- $A_{11z} = \frac{1}{6}z_q - \frac{4}{3}z_u - \frac{1}{3}z_d + \frac{1}{2}z_\ell - z_e = 0$.

We can directly simplify the contribution of the hypercharges using the usual argument and we are left with

$$A_{11z} = \frac{1}{6}\epsilon - \frac{4}{3}\epsilon - \frac{1}{3}\epsilon + \frac{1}{2}\epsilon - \epsilon = -2\epsilon \quad (27)$$

that is again satisfied if $\epsilon = 0$.

- $A_{GGz} = 2z_\ell - z_e - z_\nu = 0$.

The usual reasoning implies that this condition is automatically satisfied.

We now turn to the two non linear equations introducing the notation $\epsilon^{(2)} = \sum_{i=1}^3 \epsilon_i^2$ and

$\epsilon^{(3)} = \sum_{i=1}^3 \epsilon_i^3$. Let us point out the following relations:

$$z_f^{(2)} = \sum_{i=1}^3 z_{f_i}^2 = \sum_{i=1}^3 (y_f + \epsilon_i)^2 = \sum_{i=1}^3 y_f^2 + 2y_f \sum_{i=1}^3 \epsilon_i + \sum_{i=1}^3 \epsilon_i^2 = 3y_f^2 + 2y_f\epsilon + \epsilon^{(2)}, \quad (28)$$

$$\begin{aligned} z_f^{(3)} &= \sum_{i=1}^3 z_{f_i}^3 = \sum_{i=1}^3 (y_f + \epsilon_i)^3 = \sum_{i=1}^3 y_f^3 + 3y_f \sum_{i=1}^3 \epsilon_i^2 + 3y_f^2 \sum_{i=1}^3 \epsilon_i + \sum_{i=1}^3 \epsilon_i^3 \\ &= 3y_f^3 + 3y_f\epsilon^{(2)} + 3y_f^2\epsilon + \epsilon^{(3)}, \end{aligned} \quad (29)$$

and consider the l.h.s of (13). Using (28) and considering that the ϵ -independent terms amount to the contribution of the hypercharge and therefore give zero, we have

$$\begin{aligned} A_{1zz} &= (2y_q\epsilon + \epsilon^{(2)}) - 2(2y_u\epsilon + \epsilon^{(2)}) + (2y_d\epsilon + \epsilon^{(2)}) - [(2y_\ell\epsilon + \epsilon^{(2)}) - (2y_\nu\epsilon + \epsilon^{(2)})] \\ &= \epsilon([2y_q - 4y_u + 2y_d] - 2[y_\ell - y_\nu]) + \epsilon^{(2)}(1 - 2 + 1 - 1 + 1) = 0. \end{aligned} \quad (30)$$

Indeed, the first term vanishes because from the linear equations $\epsilon = 0$, and the second one is zero because the coefficients sum to zero.

Finally, let us consider $A_{zzz} = 3[2z_q^{(3)} - z_u^{(3)} - z_d^{(3)}] + [2z_\ell^{(3)} - z_\nu^{(3)} - z_e^{(3)}]$. Using (29), cancelling the ϵ -independent terms and those proportional to ϵ we are left with

$$\begin{aligned} A_{zzz} &= 3 \left[2(3y_q \epsilon^{(2)} + \epsilon^{(3)}) - (3y_u \epsilon^{(2)} + \epsilon^{(3)}) - (3y_d \epsilon^{(2)} + \epsilon^{(3)}) \right] \\ &\quad + 2(3y_\ell \epsilon^{(2)} + \epsilon^{(3)}) - (3y_e \epsilon^{(2)} + \epsilon^{(3)}) - (3y_\nu \epsilon^{(2)} + \epsilon^{(3)}) \\ &= 3\epsilon^{(2)} \left[3(2y_q - y_u - y_d) + 2y_\ell - y_e - y_\nu \right] + \epsilon^{(3)} [3(2 - 1 - 1) + 2 - 1 - 1] = 0. \end{aligned} \quad (31)$$

This holds because the coefficients of $\epsilon^{(2)}$ and $\epsilon^{(3)}$ vanish, as one can verify using (4) in the case of the coefficient of $\epsilon^{(2)}$ and evidently for the coefficient of $\epsilon^{(3)}$.

Until now we worked in the flavour basis but for phenomenology we have to rotate fermions to the mass eigenstate basis.

3.2 Rotation of fermions to the mass eigenstate basis

3.2.1 General formulation

We denote fermion mass matrices in the flavour basis by \hat{M}_ψ treating neutrinos as Dirac particles. Diagonalizing them by unitarity matrices V_L^ψ and V_R^ψ as follows

$$(\hat{M}_\psi)_D = (V_L^\psi)^\dagger \hat{M}_\psi V_R^\psi, \quad (32)$$

we find the familiar CKM [24, 25] and PMNS [26, 27] matrices

$$V_{\text{CKM}} = (V_L^u)^\dagger V_L^d, \quad U_{\text{PMNS}} = (V_L^e)^\dagger V_L^\nu. \quad (33)$$

Note the difference in the common definition of the PMNS matrix relative to the CKM matrix, so that in fact U_{PMNS}^\dagger corresponds to the CKM matrix.

Next, in the presence of flavour non-universal Z' couplings, flavour-violating Z' couplings are generated in the fermion mass eigenstate basis so that instead of (2) we have now [4]

$$\Delta_L^{ij}(Z') = g_{Z'} B_L^{ij}(\psi_L), \quad \Delta_R^{ij}(Z') = g_{Z'} B_R^{ij}(\psi_R), \quad (34)$$

where

$$B_L^{ij}(\psi_L) = [(V_L^\psi)^\dagger \hat{Z}_L^\psi V_L^\psi]^{ij}, \quad B_R^{ij}(\psi_R) = [(V_R^\psi)^\dagger \hat{Z}_R^\psi V_R^\psi]^{ij}. \quad (35)$$

$\hat{Z}_{\psi,L}$ and $\hat{Z}_{\psi,R}$ are diagonal matrices

$$\begin{aligned} \hat{Z}_L^\psi &= \text{diag}[z_{\psi_L^1}, z_{\psi_L^2}, z_{\psi_L^3}], \\ \hat{Z}_R^\psi &= \text{diag}[z_{\psi_R^1}, z_{\psi_R^2}, z_{\psi_R^3}], \end{aligned} \quad (36)$$

with the diagonal elements composed of the $U(1)'$ charges of the SM fermions. Let us then specify these equations to the simple model in question.

3.2.2 Rotation to mass eigenstates: quarks

Let us consider the Yukawa Lagrangian for the SM fermions in the presence of a single Higgs doublet ϕ and denote with $\begin{pmatrix} U \\ D \end{pmatrix}_L$ a generic LH doublet. We have two possibilities

to build up a quantity invariant under $SU(2)$ transformations, i.e.:

$$\phi^\dagger \begin{pmatrix} U \\ D \end{pmatrix}_L, \quad \phi^T \tilde{\epsilon} \begin{pmatrix} U \\ D \end{pmatrix}_L, \quad (37)$$

where T means the transpose and $\tilde{\epsilon}$ is the totally antisymmetric tensor:

$$\tilde{\epsilon} = \begin{pmatrix} 0 & 1 \\ -1 & 0 \end{pmatrix}. \quad (38)$$

Considering explicitly the case of quarks and leptons, the Yukawa Lagrangian reads:

$$\mathcal{L}_{yuk} = \sum_{i,j=1}^3 \left\{ -(C_e)_{ij} \bar{e}_{iR} \phi^\dagger \begin{pmatrix} \nu_{e_j L} \\ e_{jL} \end{pmatrix} + (C'_q)_{ij} \bar{u}_{iR} \phi^T \tilde{\epsilon} \begin{pmatrix} u_{jL} \\ d'_{jL} \end{pmatrix} - (C_q)_{ij} \bar{d}'_{iR} \phi^\dagger \begin{pmatrix} u_{jL} \\ d'_{jL} \end{pmatrix} + \text{h.c.} \right\} \quad (39)$$

We next assume that for up-quarks flavour and mass eigenstates are equal to each other. In the SM this assumption would be immaterial because of the flavour universality of the Z^0 couplings. But for the Z' interactions it is a model assumption that in the basis in which the up-quark mass matrix is diagonal Z' couplings to up-quarks are flavour conserving. This is the simplest assumption in order to generate flavour violation mediated by a Z' in the down-quark sector which is necessary if we want to address B physics anomalies, possible ϵ'/ϵ anomaly and decays like $K^+ \rightarrow \pi^+ \nu \bar{\nu}$ and $K_L \rightarrow \pi^0 \nu \bar{\nu}$.

For the time being we indicate by a prime that the down-type quarks are at this stage still in the flavour basis before they will be rotated to mass eigenstates. \mathcal{L}_{yuk} is invariant under $U(1)'$ if the z -charges satisfy for each generation ($i = 1, 2, 3$) the requirements:

$$\begin{aligned} z_H &= z_{q_i} - z_{d_i}, \\ z_H &= z_{u_i} - z_{q_i}, \\ z_H &= z_{\ell_i} - z_{e_i}, \end{aligned} \quad (40)$$

where z_H denotes the Higgs $U(1)'$ -charge. Recalling that in our model the fermion z -charges are given by $z_{f_i} = y_f + \epsilon_i$, if we fix $z_H = y_H$, i.e. the Higgs SM hypercharge, we see that the relations (40) are automatically satisfied because the Yukawa Lagrangian is invariant under the SM gauge group $U(1)_Y$. For example, to demonstrate this explicitly, we consider the first generation. Then: $z_{d_1} = y_d + \epsilon_1$, $z_{q_1} = y_q + \epsilon_1$ so that the first equation in (40) is $z_{q_1} - z_{d_1} = y_q + \epsilon_1 - y_d - \epsilon_1 = y_q - y_d = y_H = z_H$.

In order to find the interactions of the Z' in the quark mass eigenstate basis we assume, as stated above, $V_L^u = \hat{1}$ and $V_R^u = \hat{1}$ and concentrate our discussion on the down quarks that are rotated as follows

$$\begin{pmatrix} d' \\ s' \\ b' \end{pmatrix}_L = V_{\text{CKM}} \begin{pmatrix} d \\ s \\ b \end{pmatrix}_L, \quad \begin{pmatrix} d' \\ s' \\ b' \end{pmatrix}_R = V_R^d \begin{pmatrix} d \\ s \\ b \end{pmatrix}_R. \quad (41)$$

In writing the first equation we used the fact that in the up-basis¹ we have $V_L^u = \hat{1}$ and consequently $V_L^d = V_{\text{CKM}}$ as seen in (33). V_R^d is a unitary matrix which although present

¹See for example [28, 29] for a discussion on basis definitions of Wilson coefficients.

in the SM, does not appear in the SM interactions because of the absence of RH charged currents in the SM and flavour universality of RH Z^0 couplings.

Recalling that

$$\hat{Z}_L^d = \text{diag}[z_{q_1}, z_{q_2}, z_{q_3}], \quad \hat{Z}_R^d = \text{diag}[z_{d_1}, z_{d_2}, z_{d_3}], \quad (42)$$

we find for $i \neq j$

$$\Delta_L^{ij}(Z', d_L) = g_{Z'} \sum_{\alpha=1}^3 \epsilon_\alpha [\lambda_{u_\alpha}^{(ij)}]_L, \quad \Delta_R^{ij}(Z', d_R) = g_{Z'} \sum_{\alpha=1}^3 \epsilon_\alpha [\lambda_{u_\alpha}^{(ij)}]_R, \quad (43)$$

where the parameters $[\lambda_{u_\alpha}^{(ij)}]_{L,R}$ denote

$$[\lambda_{u_\alpha}^{(ij)}]_L = (V_{\text{CKM}})^*_{u_\alpha i} (V_{\text{CKM}})_{u_\alpha j}, \quad [\lambda_{u_\alpha}^{(ij)}]_R = (V_R^d)^*_{u_\alpha i} (V_R^d)_{u_\alpha j}. \quad (44)$$

It should be noted that the terms in the z_i -charges involving hypercharges disappeared because of their flavour universality. Furthermore, the parameters ϵ_α are the same in the LH and RH couplings, a specific property of our model. We recall that the cancellation of gauge anomalies requires their sum to vanish so that

$$\boxed{\epsilon_3 = -\epsilon_1 - \epsilon_2}, \quad (45)$$

with $\epsilon_{1,2}$ being real rational numbers.

Adopting the standard CKM phase convention, where the 5 relative phases of the quark fields are adjusted to remove 5 complex phases from the CKM matrix, we have no more freedom to remove the 6 complex phases from V_R^d . In the standard CKM basis V_R^d can then be parametrised as follows [30, 31]

$$V_R^d = D_U V_R^0 D_D^\dagger, \quad (46)$$

where V_R^0 is a ‘‘CKM-like’’ mixing matrix, containing only three real mixing angles and one non-trivial phase. The diagonal matrices $D_{U,D}$ contain the remaining CP-violating phases. Choosing the standard parametrisation for V_R^0 we have

$$V_R^0 = \begin{pmatrix} \tilde{c}_{12}\tilde{c}_{13} & \tilde{s}_{12}\tilde{c}_{13} & \tilde{s}_{13}e^{-i\phi} \\ -\tilde{s}_{12}\tilde{c}_{23} - \tilde{c}_{12}\tilde{s}_{23}\tilde{s}_{13}e^{i\phi} & \tilde{c}_{12}\tilde{c}_{23} - \tilde{s}_{12}\tilde{s}_{23}\tilde{s}_{13}e^{i\phi} & \tilde{s}_{23}\tilde{c}_{13} \\ \tilde{s}_{12}\tilde{s}_{23} - \tilde{c}_{12}\tilde{c}_{23}\tilde{s}_{13}e^{i\phi} & -\tilde{s}_{23}\tilde{c}_{12} - \tilde{s}_{12}\tilde{c}_{23}\tilde{s}_{13}e^{i\phi} & \tilde{c}_{23}\tilde{c}_{13} \end{pmatrix}, \quad (47)$$

and

$$D_U = \text{diag}(1, e^{i\phi_2^u}, e^{i\phi_3^u}), \quad D_D = \text{diag}(e^{i\phi_1^d}, e^{i\phi_2^d}, e^{i\phi_3^d}). \quad (48)$$

Inserting these formulae into (43) results in flavour violating Z' couplings to down-quarks. The flavour-conserving ones are modified by the rotations and can be obtained from (34). But the expressions for them are not transparent. In order to improve on this we will assume in what follows that the \tilde{s}_{ij} in the matrix (47) are very small and adopt the simplifying approximation of setting to 1 the cosines and retaining only terms linear in \tilde{s}_{ij} .

Exploiting then CKM unitarity and the relation (45) we find the following formulae for the Z' couplings that will govern our numerical analysis in Section 5.

LH couplings: $i = d, s, b$

$$\Delta_L^{ij}(Z') = g_{Z'}[(2\epsilon_1 + \epsilon_2)V_{uj}V_{ui}^* + (\epsilon_1 + 2\epsilon_2)V_{cj}V_{ci}^*], \quad i \neq j \quad (49)$$

$$\Delta_L^{ii}(Z') = g_{Z'}\left[\frac{1}{6} + (2\epsilon_1 + \epsilon_2)|V_{ui}|^2 + (\epsilon_1 + 2\epsilon_2)|V_{ci}|^2 - \epsilon_1 - \epsilon_2\right], \quad (50)$$

RH couplings: $i = d, s, b$

$$\Delta_R^{sd}(Z') = g_{Z'} e^{i\phi_K} \tilde{s}_{12} (\epsilon_1 - \epsilon_2), \quad (51)$$

$$\Delta_R^{bd}(Z') = g_{Z'} e^{i\phi_d} \tilde{s}_{13} (2\epsilon_1 + \epsilon_2), \quad (52)$$

$$\Delta_R^{bs}(Z') = g_{Z'} e^{i\phi_s} \tilde{s}_{23} (\epsilon_1 + 2\epsilon_2), \quad (53)$$

$$\Delta_R^{ii}(Z') = g_{Z'}\left[-\frac{1}{3} + \epsilon_i\right], \quad (54)$$

where

$$\phi_K = -\phi_{1d} + \phi_{2d}, \quad (55)$$

$$\phi_d = \phi - \phi_{1d} + \phi_{3d}, \quad (56)$$

$$\phi_s = -\phi_{2d} + \phi_{3d}. \quad (57)$$

We note that the parameters (\tilde{s}_{12}, ϕ_K) enter only in the Kaon sector, (\tilde{s}_{13}, ϕ_d) only in the B_d sector, and (\tilde{s}_{23}, ϕ_s) only in the B_s sector. This division will make our numerical analysis more transparent than working directly with (47).

Finally, for up-quarks we have

$$\Delta_L^{ii}(Z') = g_{Z'}\left[\frac{1}{6} + \epsilon_i\right], \quad \Delta_R^{ii}(Z') = g_{Z'}\left[\frac{2}{3} + \epsilon_i\right], \quad (i = u, c). \quad (58)$$

3.2.3 Rotation to mass eigenstates: leptons

Denoting $U_{\text{PMNS}} = U$, rotation to the mass eigenstates in the lepton sector is usually done through

$$\begin{pmatrix} \nu_e \\ \nu_\mu \\ \nu_\tau \end{pmatrix} = \begin{pmatrix} U_{e1} & U_{e2} & U_{e3} \\ U_{\mu1} & U_{\mu2} & U_{\mu3} \\ U_{\tau1} & U_{\tau2} & U_{\tau3} \end{pmatrix} \begin{pmatrix} \nu_1 \\ \nu_2 \\ \nu_3 \end{pmatrix}, \quad (59)$$

where ν_ℓ with $\ell = e, \mu, \tau$ are flavour eigenstates and ν_i , with $i = 1, 2, 3$ mass eigenstates. Comparing with the CKM matrix in (41) we note that whereas the PMNS matrix relates neutrinos in the mass and interaction (flavour) bases, the CKM matrix is doing it for down-quarks. This is only the convention used in the literature which assumes that $V_L^e = \hat{1}$ and has no impact on physics implications within the SM.

Here we prefer to consider scenarios in which $V_L^\nu = \hat{1}$, so that, the rotation is made on charged leptons instead of neutrinos. In this case we have

$$U_{\text{PMNS}} = (V_L^e)^\dagger, \quad (60)$$

and consequently instead of (59)

$$\begin{pmatrix} e' \\ \mu' \\ \tau' \end{pmatrix} = \begin{pmatrix} U_{e1}^* & U_{\mu1}^* & U_{\tau1}^* \\ U_{e2}^* & U_{\mu2}^* & U_{\tau2}^* \\ U_{e3}^* & U_{\mu3}^* & U_{\tau3}^* \end{pmatrix} \begin{pmatrix} e \\ \mu \\ \tau \end{pmatrix}. \quad (61)$$

e', μ', τ' are flavour eigenstates and e, μ, τ mass eigenstates.

We find then for $i \neq j$

$$\Delta_L^{ij}(Z', e_L) = g_{Z'} \sum_{\alpha=1}^3 \epsilon_\alpha [\lambda_{\nu_\alpha}^{(ij)}]_L, \quad \Delta_R^{ij}(Z', e_R) = g_{Z'} \sum_{\alpha=1}^3 \epsilon_\alpha [\lambda_{\nu_\alpha}^{(ij)}]_R, \quad (62)$$

where the parameters $[\lambda_{\nu_\alpha}^{(ij)}]_{L,R}$ denote:

$$[\lambda_{\nu_\alpha}^{(ij)}]_L = (U_{\text{PMNS}}^\dagger)_{i\nu_\alpha} (U_{\text{PMNS}}^\dagger)_{j\nu_\alpha}^*, \quad [\lambda_{\nu_\alpha}^{(ij)}]_R = (V_R^\epsilon)_{\nu_\alpha i}^* (V_R^\epsilon)_{\nu_\alpha j}. \quad (63)$$

The matrix V_R^ϵ is analogous to V_R^d and can be parametrized as the latter one with three new mixing angles and six complex phases.

The LH couplings to charged leptons are then given by:

LH couplings: $i = e, \mu, \tau$

$$\Delta_L^{ij}(Z') = g_{Z'} [(2\epsilon_1 + \epsilon_2)U_{i1}U_{j1}^* + (\epsilon_1 + 2\epsilon_2)U_{i2}U_{j2}^*], \quad i \neq j \quad (64)$$

$$\Delta_L^{ii}(Z') = g_{Z'} [-\frac{1}{2} + (2\epsilon_1 + \epsilon_2)|U_{i1}|^2 + (\epsilon_1 + 2\epsilon_2)|U_{i2}|^2 - \epsilon_1 - \epsilon_2]. \quad (65)$$

Similarly,

RH couplings: $i = e, \mu, \tau$

$$\Delta_R^{\mu e}(Z') = g_{Z'} e^{i\phi_{12}} \tilde{t}_{12} (\epsilon_1 - \epsilon_2), \quad (66)$$

$$\Delta_R^{\tau e}(Z') = g_{Z'} e^{i\phi_{13}} \tilde{t}_{13} (2\epsilon_1 + \epsilon_2), \quad (67)$$

$$\Delta_R^{\tau \mu}(Z') = g_{Z'} e^{i\phi_{23}} \tilde{t}_{23} (\epsilon_1 + 2\epsilon_2), \quad (68)$$

$$\Delta_R^{ii}(Z') = g_{Z'} [-1 + \epsilon_i], \quad (69)$$

where ϕ_{ij} and \tilde{t}_{ij} replace $\phi_{K,d,s}$ and \tilde{s}_{ij} of the quark sector. Thus $(\tilde{t}_{12}, \phi_{12})$ parametrize $\mu \rightarrow e$ transitions, $(\tilde{t}_{13}, \phi_{13})$ describe $\tau \rightarrow e$ transitions and $(\tilde{t}_{23}, \phi_{23})$ enter $\tau \rightarrow \mu$ ones.

Finally, for neutrinos,

$$\Delta_L^{\nu_i \nu_i}(Z') = g_{Z'} [-\frac{1}{2} + \epsilon_i], \quad (i = \nu_1, \nu_2, \nu_3). \quad (70)$$

There are no light RH neutrinos and we will assume that the RH ones are so heavy that they cannot contribute to the processes considered by us.

In order to evaluate the couplings in (64) and (65) we will use central values of the relevant entries and parameters in the PMNS matrix as resulting from the fit in [32]

$$\sin^2 \theta_{12} = 0.310, \quad \sin^2 \theta_{23} = 0.582, \quad \sin^2 \theta_{13} = 0.0224, \quad \delta = 217^\circ, \quad (71)$$

$$|U_{e1}| = 0.821, \quad |U_{e2}| = 0.550, \quad |U_{e3}| = 0.150, \quad (72)$$

$$|U_{\mu 1}| = 0.290, \quad |U_{\mu 2}| = 0.590, \quad |U_{\mu 3}| = 0.754, \quad (73)$$

$$|U_{\tau 1}| = 0.491, \quad |U_{\tau 2}| = 0.592, \quad |U_{\tau 3}| = 0.639. \quad (74)$$

The values given above satisfy the PMNS unitarity constraint within a few percent which is much less than uncertainties in separate entries.

4 Considered observables

4.1 Preliminaries

We refrain, with the exception of lepton flavour violation, from listing the formulae for observables entering our analysis as they can be found in the same notation in [3, 33, 34]. For ε'/ε we use the results obtained in [35–37]. We match the Z' model directly onto the Weak effective theory (WET) at the electroweak scale. The Wilson coefficients of the WET are then evolved to the corresponding scales via the one-loop QCD anomalous dimensions [38, 39]. In the following we report the lepton flavour violating observables used in the numerical analysis.

4.2 $\mu \rightarrow e\gamma$, $\tau \rightarrow \mu\gamma$ and $\tau \rightarrow e\gamma$

We will use the formulae of [40]. We find in the case of the $\mu \rightarrow e\gamma$ decay

$$\mathcal{B}(\mu \rightarrow e\gamma) = \frac{3(4\pi)^3\alpha}{4G_F^2} [|A_{e\mu}^M|^2 + |A_{e\mu}^E|^2], \quad (75)$$

where

$$A_{e\mu}^M = -\frac{1}{96\pi^2 M_{Z'}^2} \sum_{f=e,\mu,\tau} \left[\Delta_V^{fe*}(Z') \Delta_V^{f\mu}(Z') \left(1 - 3\frac{m_f}{m_\mu}\right) + \Delta_A^{fe*}(Z') \Delta_A^{f\mu}(Z') \left(1 + 3\frac{m_f}{m_\mu}\right) \right], \quad (76)$$

$$A_{e\mu}^E = \frac{i}{96\pi^2 M_{Z'}^2} \sum_{f=e,\mu,\tau} \left[\Delta_A^{fe*}(Z') \Delta_V^{f\mu}(Z') \left(1 - 3\frac{m_f}{m_\mu}\right) + \Delta_V^{fe*}(Z') \Delta_A^{f\mu}(Z') \left(1 + 3\frac{m_f}{m_\mu}\right) \right]. \quad (77)$$

The couplings Δ_V^{ij} and Δ_A^{ij} are defined as

$$\Delta_V^{ij}(Z') = \Delta_R^{ij}(Z') + \Delta_L^{ij}(Z'), \quad \Delta_A^{ij}(Z') = \Delta_R^{ij}(Z') - \Delta_L^{ij}(Z'). \quad (78)$$

The summation is over internal charged leptons in the loop. This result is also valid for new heavy charged leptons provided $m_f/M_{Z'} \leq 0.2$. For heavier leptons exact expressions in [40] have to be used. For $\tau \rightarrow \mu\gamma$ and $\tau \rightarrow e\gamma$ obvious changes of flavour indices have to be made.

The present upper bounds read: [41]

$$\mathcal{B}(\mu \rightarrow e\gamma) \leq 4.2 \times 10^{-13}, \quad (79)$$

and [42]

$$\mathcal{B}(\tau \rightarrow \mu\gamma) \leq 4.4 \times 10^{-8}, \quad \mathcal{B}(\tau \rightarrow e\gamma) \leq 3.3 \times 10^{-8}. \quad (80)$$

4.3 Three-body Lepton decays

For a decay $\ell_j \rightarrow \ell_i \bar{\ell}_l \ell_k$ we have the following contributing operators and their Wilson coefficients with $X, Y = L, R$

$$[Q_{VXY}]_{kl}^{ij} = (\bar{\psi}_i \gamma^\mu P_X \psi_j) (\bar{\psi}_k \gamma_\mu P_Y \psi_l), \quad [C_{VXY}]_{kl}^{ij} = \frac{\Delta_X^{ij}(Z') \Delta_Y^{kl}(Z')}{M_{Z'}^2}. \quad (81)$$

Calculating the branching ratios for the most interesting decays with $k = l$ we have to take into account the presence of two identical leptons in the final state that requires the introduction of a factor $1/2$ at the level of the branching ratio. Moreover always two diagrams, differing by the interchange of identical leptons, contribute. They interfere with each other for VLL and VRR cases but not for VLR and VRL . We find then

$$\mathcal{B}(\tau^- \rightarrow \mu^- \mu^+ \mu^-) = \frac{m_\tau^5}{1536\pi^3\Gamma_\tau} [2|C_{VLL}|^2 + 2|C_{VRR}|^2 + |C_{VLR}|^2 + |C_{VRL}|^2]_{\mu\mu}^{\mu\tau}, \quad (82)$$

with analogous expressions for $\mu^- \rightarrow e^- e^+ e^-$ and $\tau^- \rightarrow e^- e^+ e^-$. Γ_τ is the total τ decay width. This formula agrees with the one in [43, 44], and can also be derived from the expressions in [45] with the factors of 2, exhibited here, hidden in the Wilson coefficients.

Present bounds are [46]:

$$\mathcal{B}(\tau^- \rightarrow \mu^- \mu^+ \mu^-) < 1.2 \cdot 10^{-8}, \quad (83)$$

$$\mathcal{B}(\tau^- \rightarrow e^- e^+ e^-) < 1.4 \cdot 10^{-8}, \quad (84)$$

$$\mathcal{B}(\mu^- \rightarrow e^- e^+ e^-) < 1.0 \cdot 10^{-12}, \quad (85)$$

that update the more conservative PDG bounds [47].

4.4 $\mu - e$ conversion in nuclei

We give next the formula for the μ - e conversion in nuclei, that is

$$\mu + (A, Z) \rightarrow e + (A, Z), \quad (86)$$

where Z and A denote the proton and atomic numbers in a nucleus, respectively. Adapting general formulae in [48] and keeping the dominant tree-level contributions we find

$$\begin{aligned} \Gamma(\mu \rightarrow e) &= \frac{\alpha^3}{16\pi^2} \frac{Z_{eff}^4}{Z} |F(q)|^2 \frac{m_\mu^5}{M_{Z'}^4} [|\Delta_L^{\mu e}(Z')|^2 + |\Delta_R^{\mu e}(Z')|^2] \\ &\times |(2Z + N)\Delta_V^{uu}(Z') + (Z + 2N)\Delta_V^{dd}(Z')|^2, \end{aligned} \quad (87)$$

with Δ_V^{ij} given in (78). Z and N denote the proton and neutron numbers in a nucleus, respectively. Z_{eff} is an effective parameter and $F(q^2)$ the nuclear form factor. The branching ratio used by experimentalists is defined by

$$\mathcal{B}(\mu \rightarrow e) = \frac{\Gamma(\mu \rightarrow e)}{\Gamma_{\text{capt}}}, \quad (88)$$

where Γ_{capt} is the muon capture rate. For the case of ${}_{22}^{48}\text{Ti}$, one finds $Z_{eff} = 17.6$ and $F(q^2 \simeq -m_\mu^2) \simeq 0.54$ [49] and $\Gamma_{\text{capt}} \simeq (2.590 \pm 0.012) \cdot 10^6/s$ [50]. The present experimental bound for the branching ratio reads [51]

$$\mathcal{B}(\mu \rightarrow e) \leq \mathcal{O}(10^{-12}). \quad (89)$$

4.5 $(g - 2)_\mu$ and $(g - 2)_e$

Using general formulae in [40] we find for $a_\mu = (g - 2)_\mu/2$

$$\Delta a_\mu(Z') \approx -\frac{1}{16\pi^2} \frac{m_\mu^2}{M_{Z'}^2} \sum_{f=e,\mu,\tau} \left[\left| \Delta_V^{f\mu}(Z') \right|^2 \left(\frac{2}{3} - \frac{m_f}{m_\mu} \right) + \left| \Delta_A^{f\mu}(Z') \right|^2 \left(\frac{2}{3} + \frac{m_f}{m_\mu} \right) \right] \quad (90)$$

with Δ_V^{ij} and Δ_A^{ij} given in (78). The summation is over internal charged leptons in the loop. This result is also valid for new heavy charged leptons provided $m_f/M_{Z'} \leq 0.2$. For heavier leptons exact expressions in [40] have to be used. For $(g - 2)_e$ one just replaces μ by e .

5 Various coupling scenarios

5.1 Preliminaries and general strategy for numerics

In Section 3 we have derived the couplings of the Z' to SM quarks and leptons as well as to RH neutrinos assuming that they are Dirac particles.

It should be recalled that the parameters ϵ_i are the same in the quark and lepton sectors which in our simple model is a direct consequence of the cancellation of gauge anomalies. This then implies that we should expect correlations between various observables not only separately within the lepton and quark systems but in particular between lepton and quark observables.

Before entering numerics it is strategically useful to count the full number of free parameters and subsequently define a few simple scenarios in which some of these parameters vanish. In this manner the number of correlations between various observables is increased.

Let us then count the number of free parameters:

- 4 real parameters entering both quark and lepton couplings

$$g_{Z'}, \quad M_{Z'}, \quad \epsilon_1, \quad \epsilon_2. \quad (91)$$

Even if all formulae listed above depend only on the ratio $g_{Z'}/M_{Z'}$, the renormalization group effects depend only on $M_{Z'}$ and these are two independent parameters.

- 1 complex phase in the PMNS matrix in LH couplings. The remaining parameters in the latter couplings are already measured parameters of the CKM and PMNS matrices.
- 3 mixing angles and three complex phases in RH quark couplings:

$$(\tilde{s}_{12}, \phi_K), \quad (\tilde{s}_{13}, \phi_d), \quad (\tilde{s}_{23}, \phi_s). \quad (92)$$

- 3 mixing angles and three complex phases in RH lepton couplings:

$$(\tilde{t}_{12}, \phi_{12}), \quad (\tilde{t}_{13}, \phi_{13}), \quad (\tilde{t}_{23}, \phi_{23}). \quad (93)$$

We observe then that in full generality we have 10 real parameters and 6 phases to our disposal. This could appear as very many. Yet, by considering K , B_d and B_s meson systems with $\Delta F = 1$ and $\Delta F = 2$ transitions and the charged lepton flavour violating

decays, $\mu - e$ conversion as well as $(g-2)_{e,\mu}$, there is a sufficient number of observables so that not only the parameters in question can be bounded but also correlations between various observables can be predicted.

In what follows, we will consider four constrained scenarios. Except for the last one, we will adopt a common strategy for numerics. We will perform a simplified analysis of $\Delta F = 2$ observables. The relevant formulae for these when a new Z' gauge boson is present can be found in Section 3.3 of [3] to which we address the reader. We consider in the Kaon sector ε_K and in the $B_{d,s}$ sectors the neutral meson mass differences $\Delta M_{d,s}$, as well, as the CP asymmetries $S_{\psi K_S}$ and $S_{\psi\phi}$ in order to identify oases in the space of new parameters discussed in the previous section for which these five observables are consistent with experiment. To this end, we set all other input parameters at their central values. But to take partially hadronic and experimental uncertainties into account we require the theory to reproduce the data for ε_K within $\pm 10\%$, $\Delta M_{s,d}$ within $\pm 5\%$ and the data on $S_{\psi K_S}$ and $S_{\psi\phi}$ within experimental 2σ . We choose a larger uncertainty for ε_K than for $\Delta M_{s,d}$ because of its strong $|V_{cb}|^4$ dependence. For the neutral Kaon mass difference ΔM_K we will only require the agreement within $\pm 25\%$ because of potential long distance uncertainties.

Specifically, our search is governed by the following allowed ranges:

$$16.0/\text{ps} \leq \Delta M_s \leq 19.5/\text{ps}, \quad 0.01 \leq S_{\psi\phi} \leq 0.10, \quad (94)$$

$$0.455/\text{ps} \leq \Delta M_d \leq 0.556/\text{ps}, \quad 0.665 \leq S_{\psi K_S} \leq 0.733. \quad (95)$$

$$0.75 \leq \frac{\Delta M_K}{(\Delta M_K)_{\text{SM}}} \leq 1.25, \quad 2.0 \times 10^{-3} \leq |\varepsilon_K| \leq 2.5 \times 10^{-3}. \quad (96)$$

Moreover, in the Kaon sector, we impose that the short-distance contribution to the $\mathcal{B}(K_L \rightarrow \mu^+ \mu^-)$ satisfies the bound [52]:

$$\mathcal{B}(K_L \rightarrow \mu^+ \mu^-)_{SD} < 2.5 \cdot 10^{-9}. \quad (97)$$

In what follows, we will first identify the region in the space of the parameters ϵ_1 and ϵ_2 allowed by the constraints in (94)-(96) for each scenario. Subsequently, we will investigate correlations between various observables in this region.

For the numerical analysis of the model of Section 3 we consider a relatively light Z' setting $M_{Z'} = 1$ TeV and we vary the gauge coupling in the range $g_{Z'} \in [0.01, 1]$. This will allow us to neglect RG effects from Yukawa and electroweak interactions that could also imply correlations between observables, thereby exhibiting the correlations implied by the cancellation of gauge anomalies. Therefore, as already stated above, the matching is performed directly onto the WET below the EW scale and only QCD RG effects are taken into account. We summarize our input in Tables 1 and 2.

5.2 Different Scenarios

We will consider a number of different scenarios that we want to describe briefly here.

5.2.1 Scenario A

In this scenario flavour violation is present only in the LH couplings. This is achieved by setting all parameters \tilde{s}_{ij} and \tilde{t}_{ij} to zero such that all flavour-violating RH couplings vanish. This leaves us with only four real parameters in (91) and the PMNS phase.

$G_F = 1.16637(1) \times 10^{-5} \text{ GeV}^{-2}$ $\sin^2 \theta_W = 0.23116(13)$	$M_Z = 91.188(2) \text{ GeV}$ $\alpha(M_Z) = 1/127.94$	$M_W = 80.385(15) \text{ GeV}$ $\alpha_s(M_Z) = 0.1184(7)$
$m_e = 0.511 \text{ MeV}$ $m_u(2 \text{ GeV}) = 2.16(11) \text{ MeV}$ $m_d(2 \text{ GeV}) = 4.68(15) \text{ MeV}$	$m_\mu = 105.66 \text{ MeV}$ $m_c(m_c) = 1.279(13) \text{ GeV}$ $m_s(2 \text{ GeV}) = 93.8(24) \text{ MeV}$	$m_\tau = 1776.9(1) \text{ MeV}$ $m_t(m_t) = 163(1) \text{ GeV}$ $m_b(m_b) = 4.19_{-0.06}^{+0.18} \text{ GeV}$
$m_{K^\pm} = 493.68(2) \text{ MeV}$ $m_{B_d} = 5279.62(15) \text{ MeV}$	$m_{K^0} = 497.61(1) \text{ MeV}$ $m_{B_s} = 5366.82(22) \text{ MeV}$	
$\Delta M_K = 0.5292(9) \times 10^{-2} \text{ ps}^{-1}$ $ \epsilon_K = 2.228(11) \times 10^{-3}$ $\sin^2(\theta_{12}) = 0.307 \pm 0.013$	$\Delta M_d = 0.5055(20) \text{ ps}^{-1}$ $S_{\psi K_S} = 0.699(17)$ $\sin^2(\theta_{23}) = 0.506 \pm 0.04$	$\Delta M_s = 17.757(21) \text{ ps}^{-1}$ $S_{\psi\phi} = 0.054(20)$ $\sin^2(\theta_{13}) = 0.0212 \pm 0.0008$

Table 1: Values of theoretical quantities used for the numerical analysis.

$F_{B_d} = 190.5(13) \text{ MeV}$ $\hat{B}_{B_d} = 1.232(53)$ $F_{B_d} \sqrt{\hat{B}_{B_d}} = 210.6(55) \text{ MeV}$ $\eta_{cc} = 1.87(76)$ $\eta_B = 0.55(1)$ $ V_{us} = 0.2254(4)$	$F_{B_s} = 230.7(12) \text{ MeV}$ $\hat{B}_{B_s} = 1.222(61)$ $F_{B_s} \sqrt{\hat{B}_{B_s}} = 256.1(57) \text{ MeV}$ $\eta_{ct} = 0.496(47)$ $\phi_\epsilon = 43.51(5)^\circ$ $ V_{ub}^{\text{nom}} = 3.7 \times 10^{-3}$	$F_K = 156.1(11) \text{ MeV}$ $\hat{B}_K = 0.766(10)$ $\xi = 1.21(2)$ $\eta_{tt} = 0.5765(65)$ $\kappa_\epsilon = 0.94(2)$ $ V_{cb}^{\text{nom}} = 42.0 \times 10^{-3}$
--	---	---

Table 2: Numerical values used for the numerical analysis.

It should be noted that the flavour conserving RH couplings are generally non-zero. In fact inspecting the formulae for these couplings, it is clear that it is impossible to set them all to zero.

There are two important implications of this structure:

- The absence of RH flavour-violating couplings implies the absence of left-right operators contributing to $\Delta F = 2$ processes. As the hadronic matrix elements of these operators are, in particular in the case of the $K^0 - \bar{K}^0$ system, strongly enhanced, their absence allows to satisfy constraints from ϵ_K and the mass differences ΔM_K , ΔM_d and ΔM_s easier than in the subsequent scenarios.
- Non-vanishing flavour conserving RH currents together with flavour-violating LH currents imply the presence of the dominant QCD (Q_6) and electroweak penguin (Q_8) operators contributing to ϵ'/ϵ thereby allowing to address the ϵ'/ϵ -anomaly.
- Moreover the small number of free parameters implies a number of correlations.

5.2.2 Scenarios B1 and B2

In these scenarios flavour violation is present in both LH and RH quark currents, but for leptons only in LH currents. At first sight six additional parameters in (92) enter the phenomenology. However, the presence of left-right operators implies that it is very difficult to satisfy the constraints in the $K^0 - \bar{K}^0$ mixing for $M_{Z'} = \mathcal{O}(1 \text{ TeV})$, so that, the Δ_R^{sd} coupling has to be strongly suppressed or even eliminated. This can be done by setting

- $\tilde{s}_{12} = 0,$ (Scenario B1) (98)

or

- $\epsilon_1 = \epsilon_2,$ (Scenario B2). (99)

In both scenarios only four additional parameters relative to Scenario A are present. Moreover, in Scenario B2 the number of free parameters is reduced through the relation $\epsilon_1 = \epsilon_2$.

5.2.3 Scenario C

In this scenario, with both LH and RH currents, it is possible, as explained in the Appendix A, to eliminate $\Delta F = 2$ constraints in Kaon and $B_{s,d}$ systems which allows to obtain larger NP effects in $\Delta F = 1$ transitions. This allows to see the correlations between various observables in different systems even better than in the previous scenarios.

6 Numerical Analysis

6.1 Results in Scenario A

The impact of the constraints (94)-(96) on the parameter space in this scenario can be deduced from Fig. 1. In the left plot, we show the allowed ranges in the (ϵ_1, ϵ_2) space resulting separately from $\Delta F = 2$ constraints in the B_d, B_s, K systems, respectively. The relations (94) and (95) produce the blue and pink overlapping regions, while the constraints in (96) significantly restrict such a space to the green zone, that we display enlarged in the right panel. The impact on the observables related to the B_d and B_s

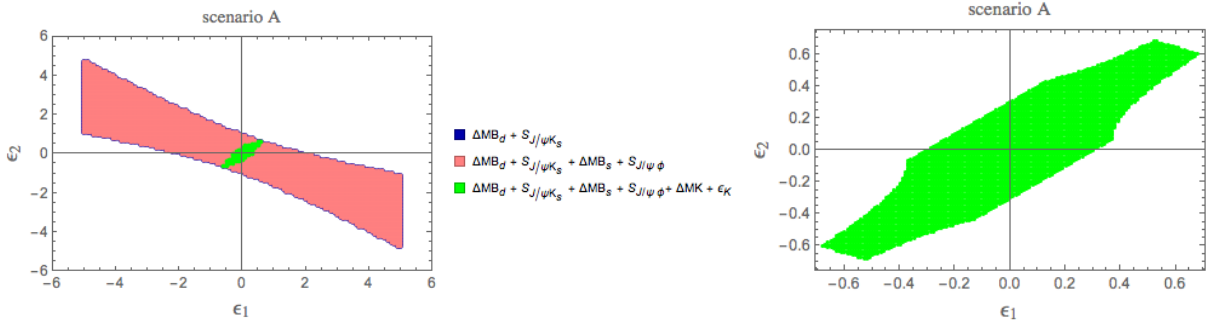


Figure 1: Scenario A. Left panel: Allowed region in the (ϵ_1, ϵ_2) plane, after imposing $\Delta F = 2$ constraints, as indicated in the legend. Right panel: Zoom of the green zone in the left panel.

system is small. For example, we find that effects on $\mathcal{B}(B_d \rightarrow \mu^+ \mu^-)$ and $\bar{\mathcal{B}}(B_s \rightarrow \mu^+ \mu^-)$ are at most 2% in this scenario, while effects on the Wilson coefficients C_9 and C_{10} entering in the description of rare $b \rightarrow s$ decays are negligible. For this reason, we do not show the corresponding plots. As for Kaon decays, while effects on $K_L \rightarrow \pi^0 \nu \bar{\nu}$ are tiny, significant deviations from the SM at the level of 20% are still allowed for $K^+ \rightarrow \pi^+ \nu \bar{\nu}$

by $\Delta F = 2$ constraints, as can be observed from Fig. 2. This scenario does not predict an enhancement of $|\varepsilon'/\varepsilon|$ with respect to the SM prediction: the largest deviation from the SM is $\simeq 2 \cdot 10^{-5}$, two orders of magnitude below its experimental value.

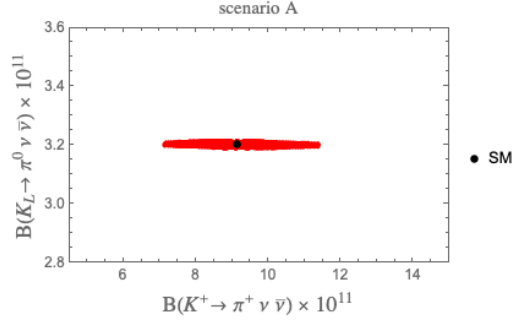


Figure 2: Scenario A. Correlation between $\mathcal{B}(K_L \rightarrow \pi^0 \nu \bar{\nu})$ and $\mathcal{B}(K^+ \rightarrow \pi^+ \nu \bar{\nu})$. The black dot represents the central value of the SM prediction.

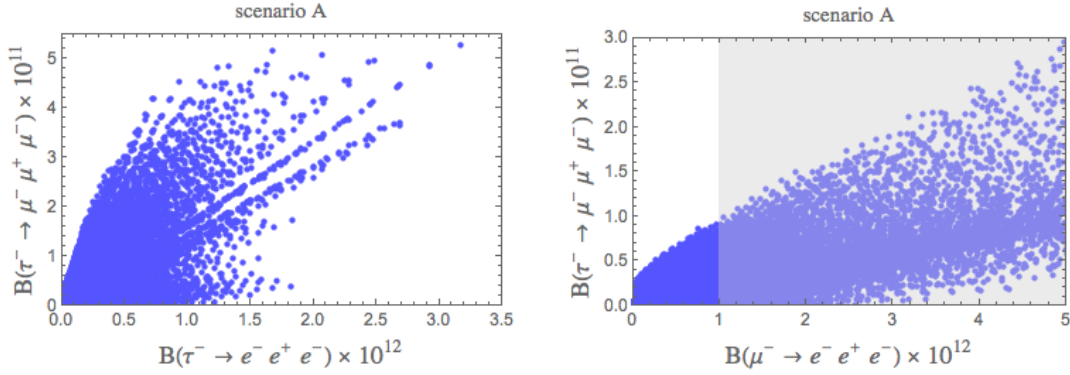


Figure 3: Scenario A. Correlation between $\mathcal{B}(\tau^- \rightarrow \mu^- \mu^+ \mu^-)$ and $\mathcal{B}(\tau^- \rightarrow e^- e^+ e^-)$ (left panel) and between $\mathcal{B}(\tau^- \rightarrow \mu^- \mu^+ \mu^-)$ and $\mathcal{B}(\mu^- \rightarrow e^- e^+ e^-)$ (right panel). The gray shaded region in the right panel is excluded by the experimental bound $\mathcal{B}(\mu^- \rightarrow e^- e^+ e^-) < 1 \cdot 10^{-12}$.

Fig. 3 displays the results for flavour violating lepton decays. The left panel shows that τ decays are predicted well below the experimental upper bounds in (83)-(84). On the other hand, $\mathcal{B}(\mu^- \rightarrow e^- e^+ e^-)$ shown in the right panel can easily be close to the experimental bound (85) and even exceed it.

Also $\mathcal{B}(\mu^- \rightarrow e^- \gamma)$ is predicted below the bound in (79), as can be inferred from the upper right panel in Fig. 4. In this figure, we display the correlations among lepton decays $\mu^- \rightarrow e^- e^+ e^-$, $\mu^- \rightarrow e^- \gamma$ and the mode $K^+ \rightarrow \pi^+ \nu \bar{\nu}$. The upper panels show, that in this scenario, the experimental bound on both leptonic decays have no impact on the possibility that $\mathcal{B}(K^+ \rightarrow \pi^+ \nu \bar{\nu})$ could significantly deviate from its SM value. On the other hand, the bound on $\mathcal{B}(\mu^- \rightarrow e^- e^+ e^-)$ reduces the allowed range for $\mathcal{B}(\mu^- \rightarrow e^- \gamma)$ (lower panel); however, this branching ratio is much smaller than the experimental upper bound, as already observed.

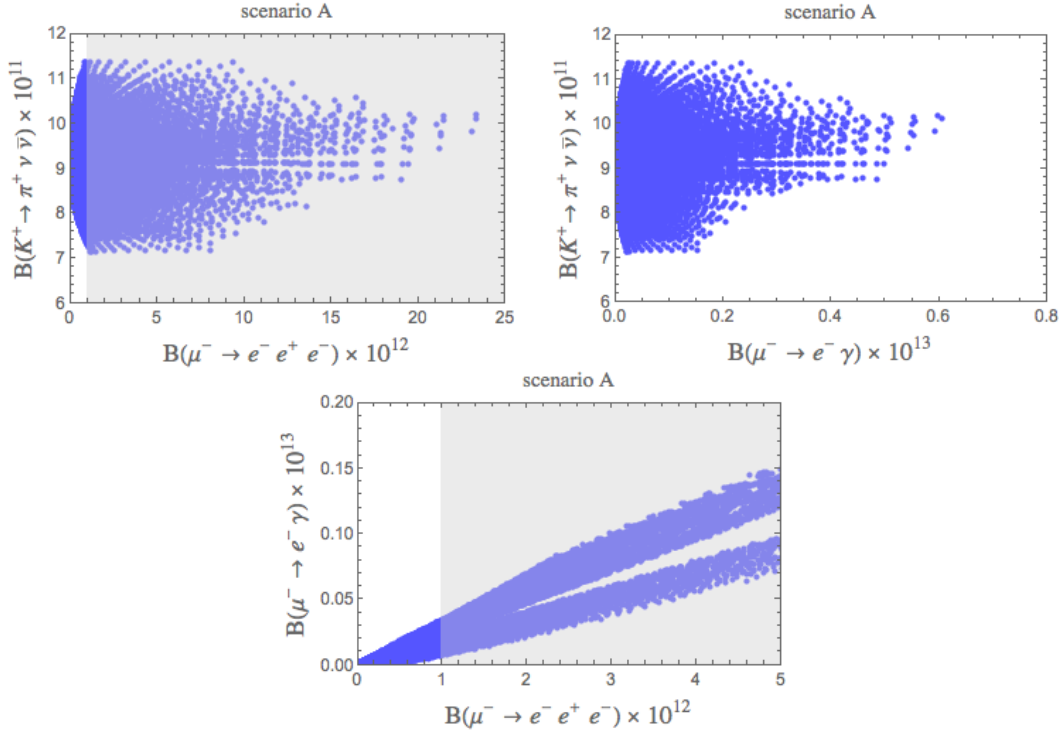


Figure 4: Scenario A. Correlation between $\mathcal{B}(K^+ \rightarrow \pi^+ \nu \bar{\nu})$ and $\mathcal{B}(\mu^- \rightarrow e^- e^+ e^-)$ (upper left panel) and between $\mathcal{B}(K^+ \rightarrow \pi^+ \nu \bar{\nu})$ and $\mathcal{B}(\mu^- \rightarrow e^- \gamma)$ (upper right panel). Correlation between $\mathcal{B}(\mu^- \rightarrow e^- \gamma)$ and $\mathcal{B}(\mu^- \rightarrow e^- e^+ e^-)$ (lower panel). The gray shaded regions are excluded by the experimental bound $\mathcal{B}(\mu^- \rightarrow e^- e^+ e^-) < 1 \cdot 10^{-12}$.

Comparing Fig. 5 with Fig. 2 we observe that the upper bound on $\mu - e$ conversion in the ballpark of 10^{-12} reduces significantly the allowed range for $\mathcal{B}(K^+ \rightarrow \pi^+ \nu \bar{\nu})$. On the other hand, as seen in this figure it has presently no impact on the allowed range for $\mu^- \rightarrow e^- e^+ e^-$. This is also the case of $\mu^- \rightarrow e^- \gamma$ not shown here.

6.2 Results in Scenario B1

The result of the subsequent application of the constraints (94)-(96) is shown in the upper panel of Fig. 6.

At odds with the previous scenario, in this case one can have significant deviations from the SM predictions in $B_{d,s}$ observables. This is for instance the case for the rare decays $B_{d,s} \rightarrow \mu^+ \mu^-$. As Fig. 7 (left panel) shows, the branching ratios of these modes can largely deviate from the SM results whose central values are represented by the black dot in that figure.

The most recent averages from the data of CMS, LHCb and ATLAS [53–56] have been presented in [23] with the result

$$\bar{\mathcal{B}}(B_s \rightarrow \mu^+ \mu^-) = (2.71 \pm 0.40) \times 10^{-9}, \quad \mathcal{B}(B_d \rightarrow \mu^+ \mu^-) = (1.01 \pm 0.81) \times 10^{-10}. \quad (100)$$

In the case of $B_s \rightarrow \mu^+ \mu^-$, we observe a departure of the data from the SM prediction

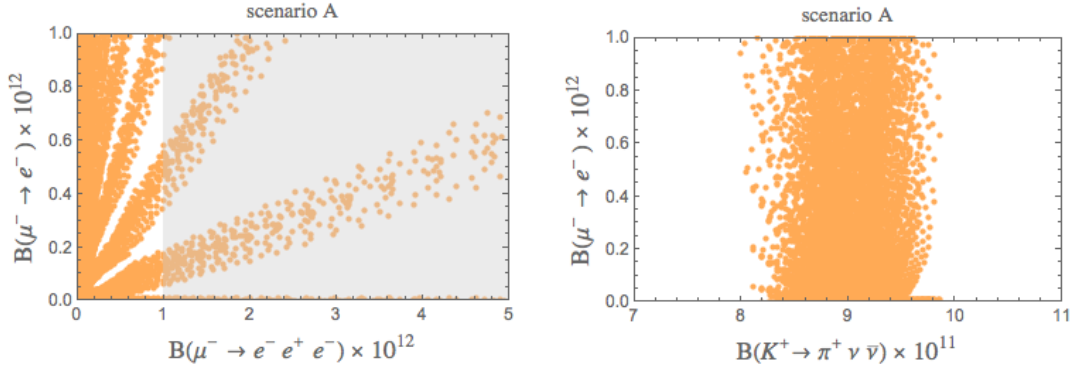


Figure 5: Scenario A. Correlation between $\mathcal{B}(\mu^- \rightarrow e^-)$ and $\mathcal{B}(\mu^- \rightarrow e^- e^+ e^-)$ (left panel). The gray shaded region is excluded by the experimental bound $\mathcal{B}(\mu^- \rightarrow e^- e^+ e^-) < 1 \cdot 10^{-12}$. Correlation between $\mathcal{B}(\mu^- \rightarrow e^-)$ and $\mathcal{B}(K^+ \rightarrow \pi^+ \nu \bar{\nu})$ (right panel).

by about 2σ . This favours NP scenarios in which the branching ratio for this decay is suppressed relatively to its SM value [23]

$$\bar{\mathcal{B}}(B_s \rightarrow \mu^+ \mu^-)_{\text{SM}} = (3.67 \pm 0.15) \times 10^{-9}, \quad \mathcal{B}(B_d \rightarrow \mu^+ \mu^-) = (1.14 \pm 0.12) \times 10^{-10}. \quad (101)$$

The relevant formulae for these observables when a new Z' contribution is added can be found in Section 3 of [3], as well as, those of the Wilson coefficients of the $b \rightarrow s \ell^+ \ell^-$ effective Hamiltonian that we are going to consider. Among such coefficients C_9 and C_{10} are already present in the SM, and we shall consider only the shift with respect to their SM values, denoted by C_9^{NP} and C_{10}^{NP} . C'_9 and C'_{10} are instead absent in the SM, so these represent pure NP quantities. Various analyses have been devoted to fit the Wilson coefficients in order to explain the observed anomalies in a number of $b \rightarrow s$ related observables. Among the possible solutions, it has been pointed out that a large negative value of C_9^{NP} or a large C'_9 could be effective. Our results for the various coefficients in scenario B1 are displayed in the upper panel of Fig. 8. Deviations from the SM are negligible for C_9^{NP} and C_{10}^{NP} but could be relevant in the case of C'_9 and C'_{10} and we display only them.

In the Kaon sector, we find that $\mathcal{B}(K_L \rightarrow \pi^0 \nu \bar{\nu})$ displays small deviations from the SM, while $\mathcal{B}(K^+ \rightarrow \pi^+ \nu \bar{\nu})$ can be strongly enhanced or suppressed with respect to the SM result, when $\mathcal{B}(K_L \rightarrow \pi^0 \nu \bar{\nu})$ is SM-like, while it is approximately stable on the SM value when $\mathcal{B}(K_L \rightarrow \pi^0 \nu \bar{\nu})$ deviates from the SM central value. This pattern of correlation is shown in the left panel of Fig. 9.

As for scenario A, also in B1 lepton flavour violating τ decays are predicted below the experimental upper limit, while $\mathcal{B}(\mu^- \rightarrow e^- e^+ e^-)$ can saturate or even exceed its experimental upper bound. Correlations among these modes are displayed in the upper panel of Fig. 10.

In contrast to the case of scenario A, in B1 $\mathcal{B}(\mu^- \rightarrow e^- \gamma)$ can saturate or even exceed the experimental upper bound. Correlations among the lepton observables $\mathcal{B}(\mu^- \rightarrow e^- e^+ e^-)$ or $\mathcal{B}(\mu^- \rightarrow e^- \gamma)$ and $\mathcal{B}(K^+ \rightarrow \pi^+ \nu \bar{\nu})$ are shown in Fig. 11 (upper plots). The experimental bound on $\mathcal{B}(\mu^- \rightarrow e^- \gamma)$ has no impact on the K^+ branching ratio. However, one can observe that, the bound on $\mathcal{B}(\mu^- \rightarrow e^- e^+ e^-)$ allows only the values

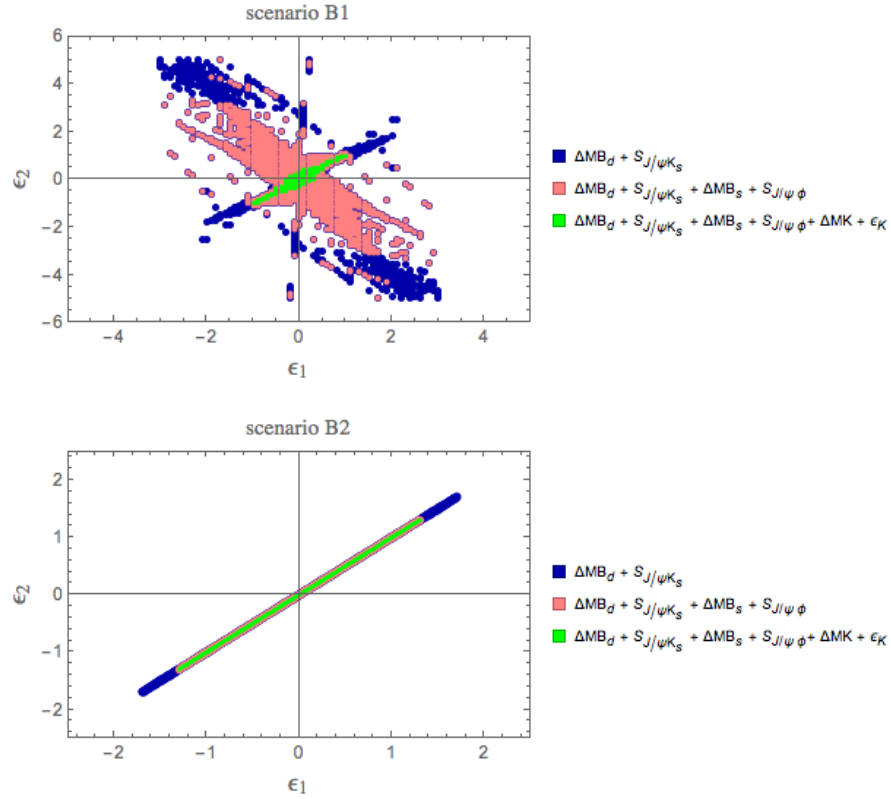


Figure 6: Scenarios B1 (upper panel) and B2 (lower panel). Allowed region in the (ϵ_1, ϵ_2) plane, after imposing $\Delta F = 2$ constraints, as indicated in the legend.

for $\mathcal{B}(K^+ \rightarrow \pi^+ \nu \bar{\nu})$ close to its SM value.

The situation is different when one considers the ratio ϵ'/ϵ and, in particular, its deviation from the SM. As the upper left panel of Fig. 12 shows, in B1 $|(\epsilon'/\epsilon)_{\text{BSM}}|$ could reach values as large as $\simeq 1.5 \cdot 10^{-4}$. However, imposing that $\mathcal{B}(\mu^- \rightarrow e^- \gamma)$ lies below its experimental upper limit, one finds that the maximum deviation in ϵ'/ϵ could be $|(\epsilon'/\epsilon)_{\text{BSM}}| \simeq 0.6 \cdot 10^{-4}$. As for the correlation between $(\epsilon'/\epsilon)_{\text{BSM}}$ and $\mathcal{B}(K^+ \rightarrow \pi^+ \nu \bar{\nu})$, from the right upper panel of Fig. 12 one can observe that deviations in one of the two observables with respect to the SM predictions exclude deviations in the other one.

But what is most important is the impact of the bounds on leptonic modes on rare B and K decay branching ratios seen already in the case of Scenario A. First one can observe from the upper plots in Fig. 13 that, even if in B1 $\bar{\mathcal{B}}(B_s \rightarrow \mu^+ \mu^-)$ can deviate significantly from its SM value, constraints in the lepton sector reduce the size of such a deviation. This is in particular the case when the bound from $\mu^- \rightarrow e^- e^+ e^-$ is applied.

But even stronger impact comes from $\mu - e$ conversion. Indeed comparing Fig. 14 with Figs. 7 and 9 we observe that the upper bound on $\mu - e$ conversion in the ballpark of 10^{-12} reduces significantly the allowed ranges for $B_s \rightarrow \mu^+ \mu^-$ and $K^+ \rightarrow \pi^+ \nu \bar{\nu}$ branching ratios. On the other hand, as seen in other plots it has presently no impact on the allowed ranges for $\mu^- \rightarrow e^- e^+ e^-$ and $\mu^- \rightarrow e^- \gamma$.

Scenario B1, similar to Scenario A shows a peculiar feature that often occurs in our model: in principle large deviations from SM predictions can be found. However, quark and lepton sector act in a complementary way to constrain each other producing

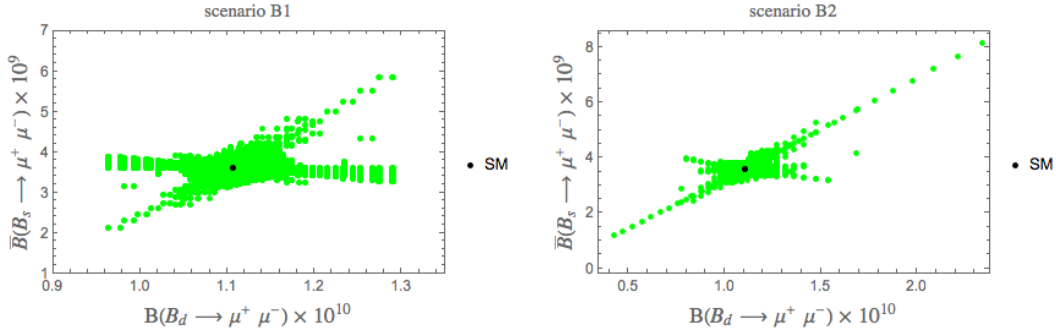


Figure 7: Scenarios B1 (left panel) and B2 (right panel). Correlation between $\mathcal{B}(B_d \rightarrow \mu^+ \mu^-)$ and $\bar{\mathcal{B}}(B_s \rightarrow \mu^+ \mu^-)$. The black dot represents the central value of the SM prediction.

observables with values close to the SM ones.

6.3 Results in Scenario B2

The parameter space in B2 is simplified because of the assumption $\epsilon_1 = \epsilon_2$, as can be observed from the lower panel in Fig. 6. As in the case of B1, also B2 displays large deviations from the SM in the $B_{d,s}$ sectors. Fig. 7 (right panel) shows that the rare decays $\mathcal{B}(B_d \rightarrow \mu^+ \mu^-)$ and $\bar{\mathcal{B}}(B_s \rightarrow \mu^+ \mu^-)$ are approximately linearly correlated, and can strongly deviate from the SM. As for the Wilson coefficients $C_9^{(\prime)}$, $C_{10}^{(\prime)}$, in B2 one finds that $\text{Im}(C_9) \simeq 0$ and $\text{Im}(C_{10}) \simeq 0$, deviations in $\text{Re}(C_9)$ and $\text{Re}(C_{10})$ are of the same size as in B1, while C_9' , C_{10}' vary in much larger ranges, as can be seen in Fig. 8 (lower plots). However, if the experimental bound on $\mathcal{B}(\mu^- \rightarrow e^- e^+ e^-)$ is imposed, these variations are practically removed as indicated by the central blue regions in Fig. 8. This is another example of the mutual role of lepton and quark sectors.

Looking at rare Kaon decays, it can be observed that for $\epsilon_1 = \epsilon_2$ the relation between $\mathcal{B}(K_L \rightarrow \pi^0 \nu \bar{\nu})$ and $\mathcal{B}(K^+ \rightarrow \pi^+ \nu \bar{\nu})$ is approximately linear. This result is displayed in the right plot in Fig. 9, which in addition shows that moderate variations with respect to the SM values are possible.

As in B1, among lepton decays the branching fractions that can be large are $\mathcal{B}(\mu^- \rightarrow e^- e^+ e^-)$, as shown by the lower plots in Fig. 10, and $\mathcal{B}(\mu^- \rightarrow e^- \gamma)$ (see lower plots in Fig. 11). Both reduce the possible range of $\mathcal{B}(K^+ \rightarrow \pi^+ \nu \bar{\nu})$, as shown in Fig. 11. They also reduce the range for $(\epsilon'/\epsilon)_{\text{BSM}}$, the impact of $\mathcal{B}(\mu^- \rightarrow e^- e^+ e^-)$ being much more constraining than that of $\mathcal{B}(\mu^- \rightarrow e^- \gamma)$, as shown in the lower left panel of Fig. 12. In B2 deviations from the SM are possible in both ϵ'/ϵ and $\mathcal{B}(K^+ \rightarrow \pi^+ \nu \bar{\nu})$ and the correlation between these two observables is shown in the right lower panel of Fig. 12.

Correlations between lepton decays and $\bar{\mathcal{B}}(B_s \rightarrow \mu^+ \mu^-)$, shown in Fig. 13, follow a pattern similar to that in B1.

In Fig. 15 we show that in this scenario NP effects in ϵ'/ϵ can be significant without having any impact on $a_{\mu,e}$. Generally the contributions of NP to $a_{\mu,e}$ are very small in all scenarios considered and this is the only figure displaying them that we show.

Similar to Scenario B1, as seen in Fig. 14, the upper bound on $\mu - e$ conversion also in this scenario has a very large impact on $K^+ \rightarrow \pi^+ \nu \bar{\nu}$ and $B_s \rightarrow \mu^+ \mu^-$.

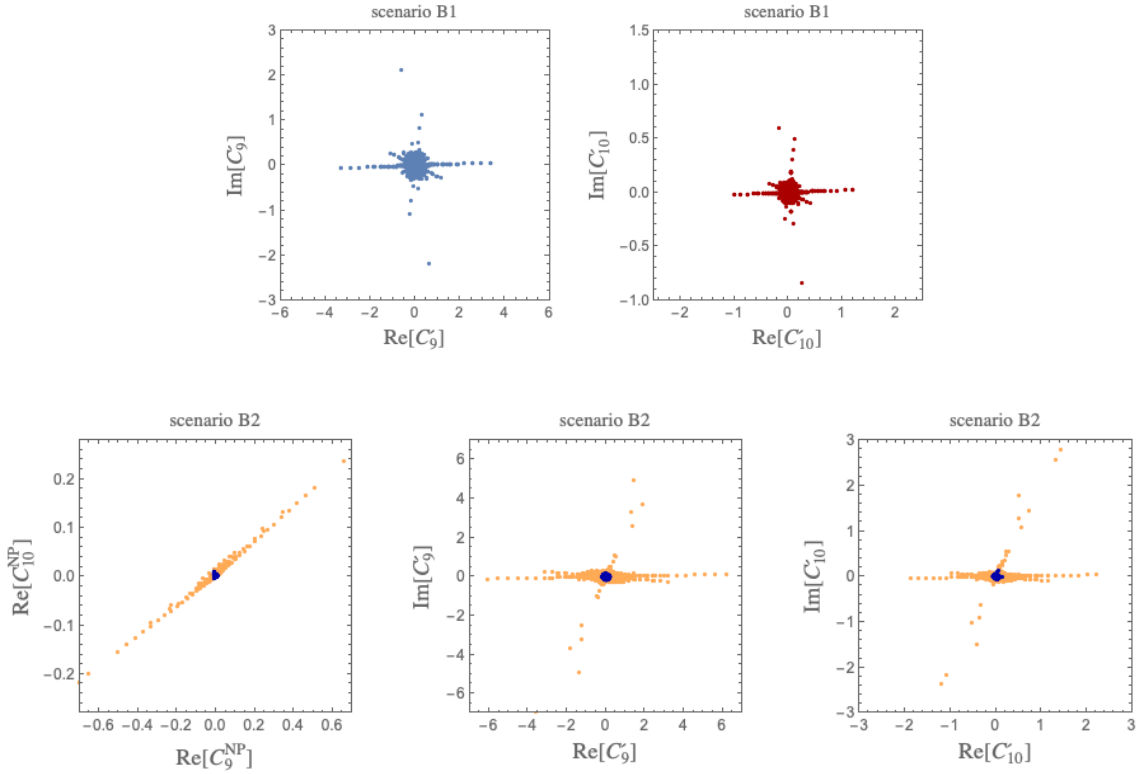


Figure 8: Scenarios B1 (upper plots) and B2 (lower plots). Wilson coefficients that appear in the $b \rightarrow s\ell^+\ell^-$ effective Hamiltonian. Only those sensibly different from zero are displayed: C_9' and C_{10}' (not present in the SM) in scenario B1 (upper plots) and in B2 (lower middle and right plots). In the case of B2 deviation from the SM value of $\text{Re}[C_9]$ and $\text{Re}[C_{10}]$ are also shown (lower left plot).

6.4 Results in Scenario C

Removing the $\Delta F = 2$ constraints using the arguments presented in the Appendix A makes NP effects much larger than in other scenarios. In this case very large NP effects in all $\Delta F = 1$ observables are possible so that hinted anomalies in various rare decays of mesons can easily be explained in the absence of pure leptonic decays. One example is shown in Fig. 16, where the branching ratios for $B_{s,d} \rightarrow \mu^+\mu^-$ decays are much more modified than in previous scenarios. Another example is shown in Fig. 17, where NP effects in $K^+ \rightarrow \pi^+\nu\bar{\nu}$ and $K_L \rightarrow \pi^0\nu\bar{\nu}$ can be very large. It is also evident that without the $K_L \rightarrow \mu^+\mu^-$ constraint NP effects would be even larger.

Yet, when the bound from $\mu - e$ conversion is taken into account the imposition of the cancellation of gauge anomalies with the help of leptons has an important impact on the allowed values of various observables in the Kaon and $B_{s,d}$ systems. Indeed the experimental bound on $\mu - e$ conversion eliminates any significant departures from the SM expectations for $K^+ \rightarrow \pi^+\nu\bar{\nu}$ and $B_{s,d} \rightarrow \mu^+\mu^-$. We show this in Fig. 18. Similar comments apply to other observables.

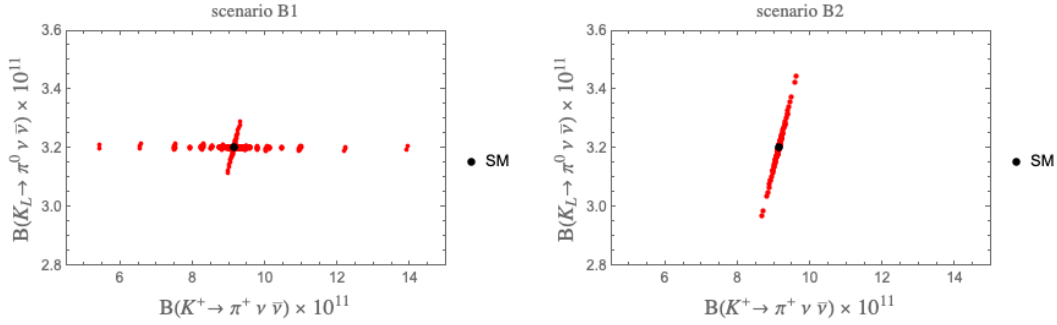


Figure 9: Scenarios B1 (left panel) and B2 (right panel). Correlation between $\mathcal{B}(K_L \rightarrow \pi^0 \nu \bar{\nu})$ and $\mathcal{B}(K^+ \rightarrow \pi^+ \nu \bar{\nu})$. The black dot represents the central value of the SM prediction.

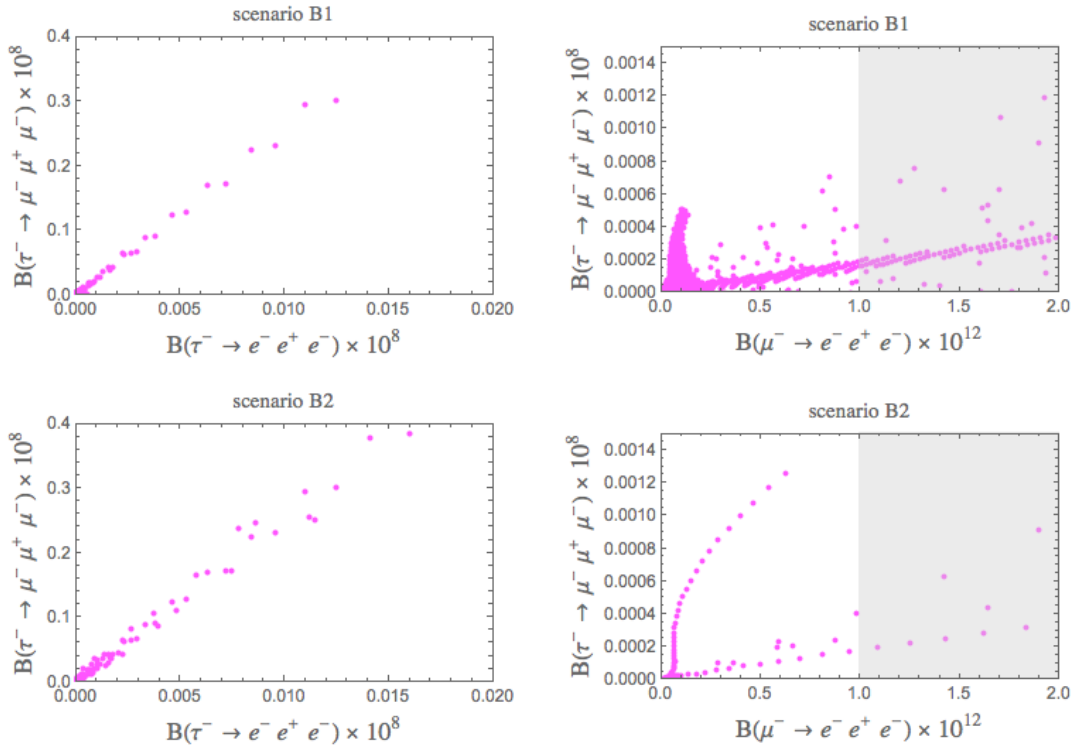


Figure 10: Scenarios B1 (upper plots) and B2 (lower plots). Correlation between $\mathcal{B}(\tau^- \rightarrow \mu^- \mu^+ \mu^-)$ and $\mathcal{B}(\tau^- \rightarrow e^- e^+ e^-)$ (left panel) and between $\mathcal{B}(\tau^- \rightarrow \mu^- \mu^+ \mu^-)$ and $\mathcal{B}(\mu^- \rightarrow e^- e^+ e^-)$ (right panel). The gray shaded region in the right panel is excluded by the experimental bound $\mathcal{B}(\mu^- \rightarrow e^- e^+ e^-) < 1 \cdot 10^{-12}$.

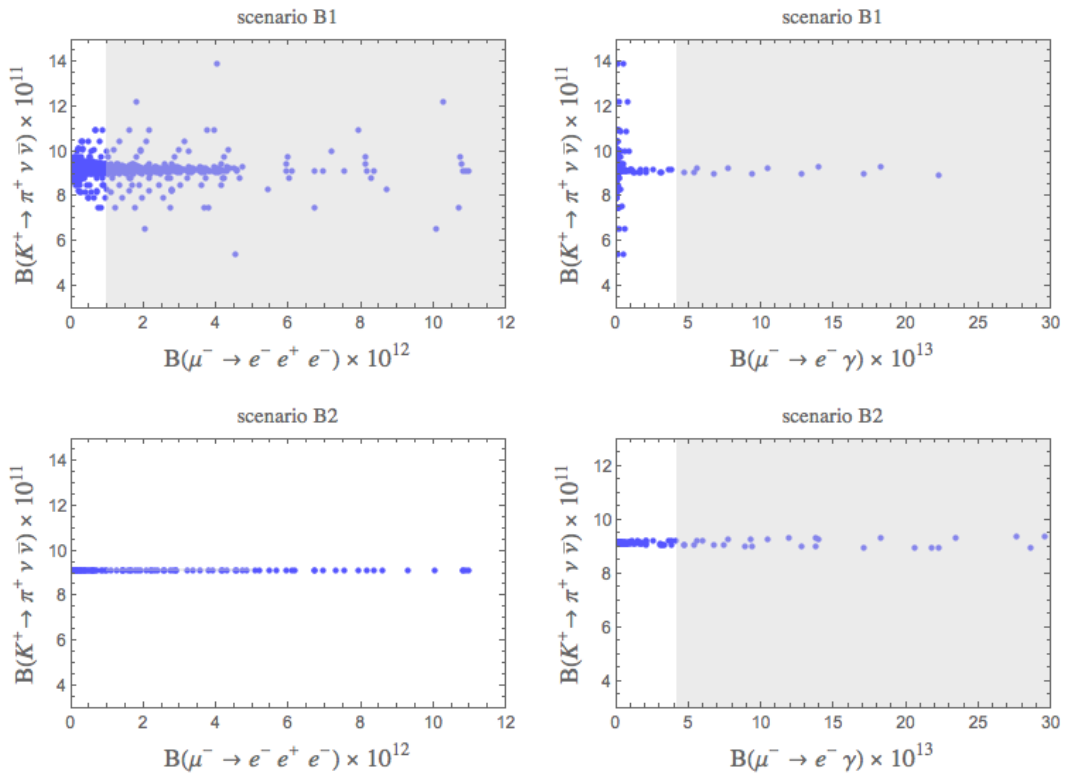


Figure 11: Scenarios B1 (upper plots) and B2 (lower plots). Correlation between $\mathcal{B}(K^+ \rightarrow \pi^+ \nu \bar{\nu})$ and $\mathcal{B}(\mu^- \rightarrow e^- e^+ e^-)$ (left panels) and between $\mathcal{B}(K^+ \rightarrow \pi^+ \nu \bar{\nu})$ and $\mathcal{B}(\mu^- \rightarrow e^- \gamma)$ (right panels). The gray shaded regions are excluded by the experimental bounds $\mathcal{B}(\mu^- \rightarrow e^- e^+ e^-) < 1 \cdot 10^{-12}$ and $\mathcal{B}(\mu^- \rightarrow e^- \gamma) < 4.2 \cdot 10^{-13}$.

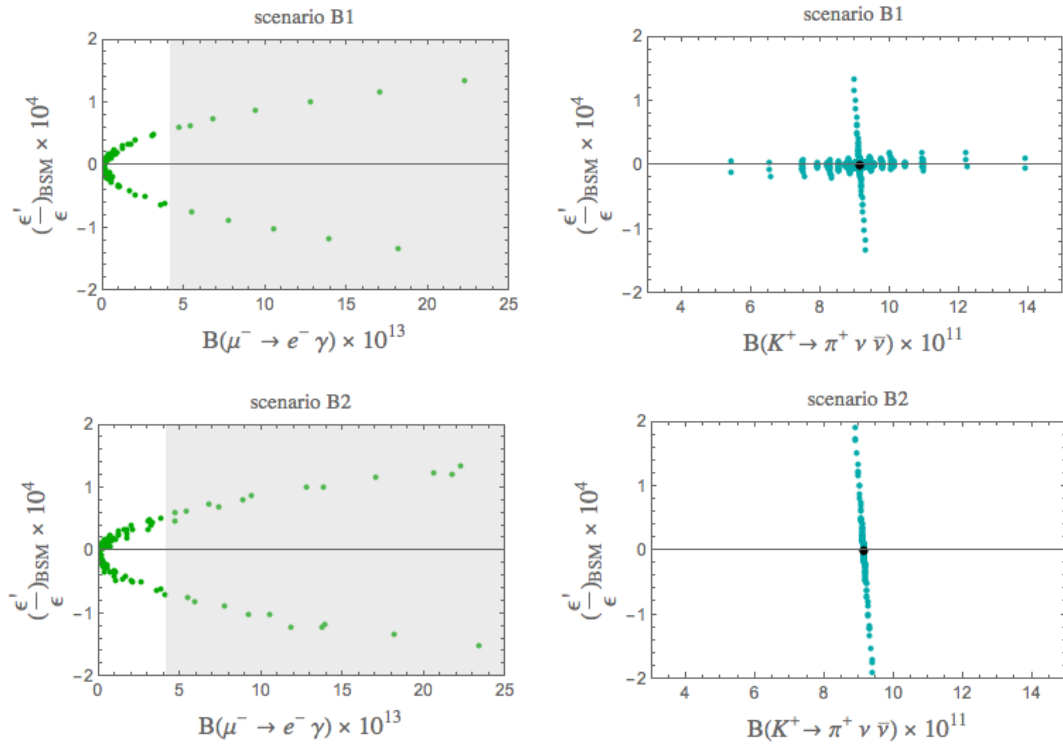


Figure 12: Scenarios B1 (upper plots) and B2 (lower plots). Correlations involving the $(\epsilon'/\epsilon)_{\text{BSM}}$ (the NP contribution to ϵ'/ϵ). Correlation with $\mathcal{B}(\mu^- \rightarrow e^- \gamma)$ (left panels) and with $\mathcal{B}(K^+ \rightarrow \pi^+ \nu \bar{\nu})$ (right panels). The gray shaded region is excluded by the experimental bound $\mathcal{B}(\mu^- \rightarrow e^- \gamma) < 4.2 \cdot 10^{-13}$.

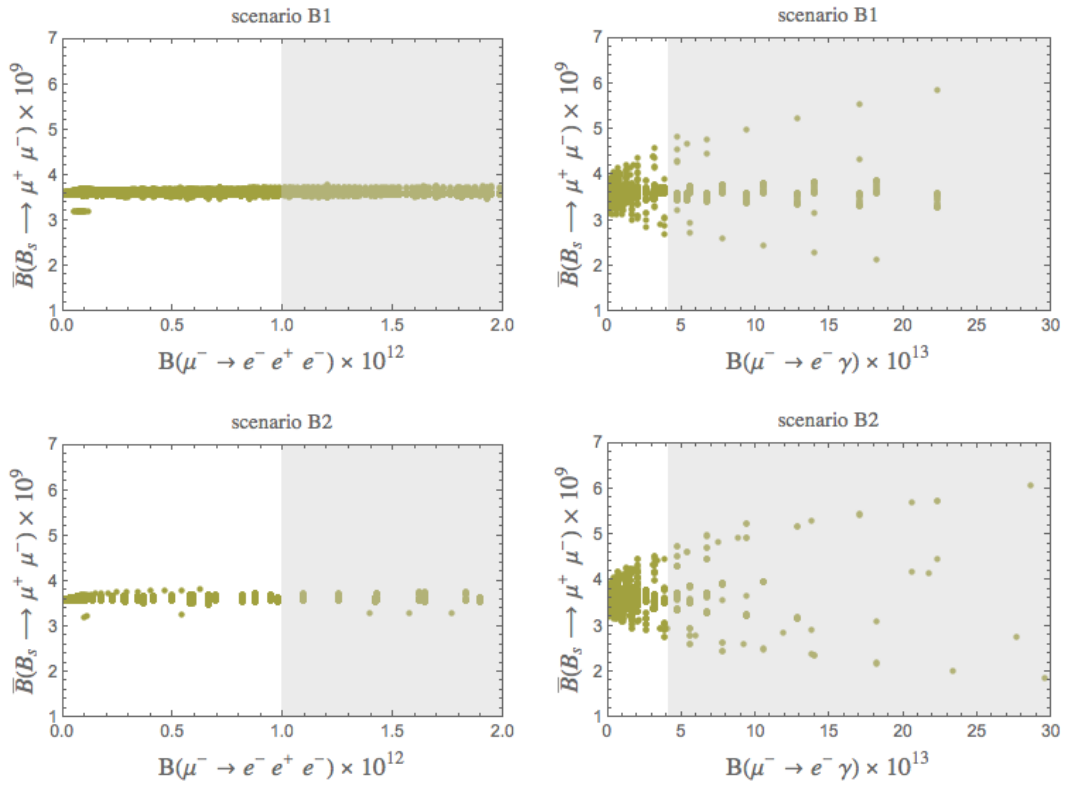


Figure 13: Scenarios B1 (upper plots) and B2 (lower plots). Correlations between $\bar{\mathcal{B}}(B_s \rightarrow \mu^+ \mu^-)$ and $\mathcal{B}(\mu^- \rightarrow e^- e^+ e^-)$ (left panels) and between $\bar{\mathcal{B}}(B_s \rightarrow \mu^+ \mu^-)$ and $\mathcal{B}(\mu^- \rightarrow e^- \gamma)$ (right panels). The gray shaded regions are excluded by the experimental bounds $\mathcal{B}(\mu^- \rightarrow e^- e^+ e^-) < 1 \cdot 10^{-12}$ and $\mathcal{B}(\mu^- \rightarrow e^- \gamma) < 4.2 \cdot 10^{-13}$.

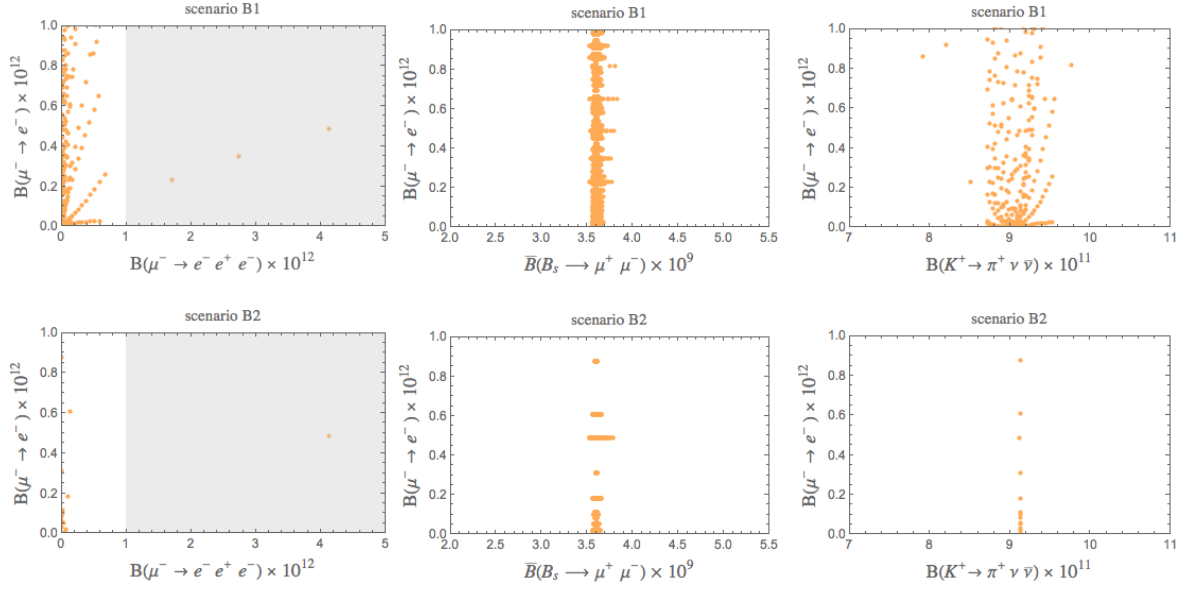


Figure 14: Scenarios B1 (upper plots) and B2 (lower plots). Correlation between $\mathcal{B}(\mu^- \rightarrow e^-)$ and $\mathcal{B}(\mu^- \rightarrow e^- e^+ e^-)$ (left panels). The gray shaded region is excluded by the experimental bound $\mathcal{B}(\mu^- \rightarrow e^- e^+ e^-) < 1 \cdot 10^{-12}$. Correlations between $\mathcal{B}(\mu^- \rightarrow e^-)$ and $\mathcal{B}(B_s \rightarrow \mu^+ \mu^-)$ (middle panels) and between $\mathcal{B}(\mu^- \rightarrow e^-)$ and $\mathcal{B}(K^+ \rightarrow \pi^+ \nu \bar{\nu})$ (right panels).

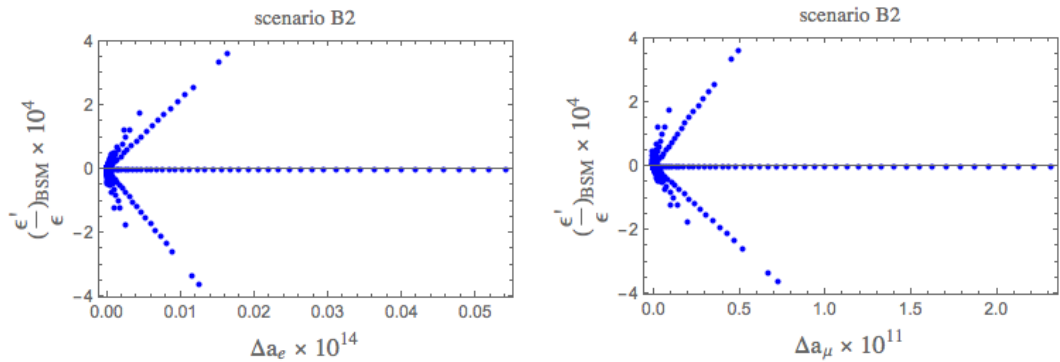


Figure 15: Scenario B2. Correlation between NP contributions to ϵ'/ϵ and a_e (left plot) and a_μ (right plot).

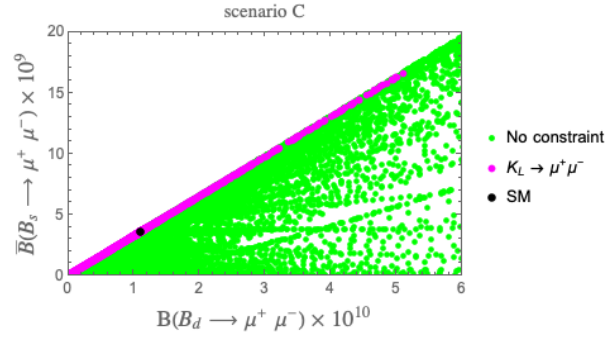


Figure 16: Scenario C. Correlation between $\mathcal{B}(B_d \rightarrow \mu^+ \mu^-)$ and $\bar{\mathcal{B}}(B_s \rightarrow \mu^+ \mu^-)$. The black dot represents the central value of the SM prediction.

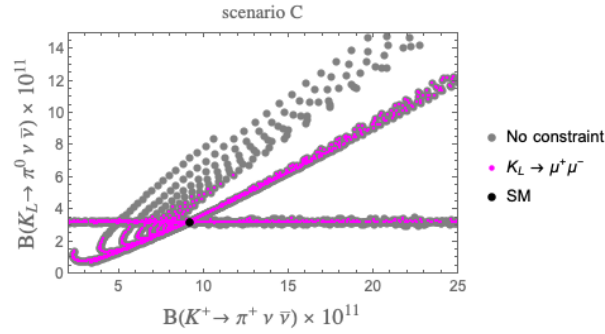


Figure 17: Scenario C. Correlation between $\mathcal{B}(K_L \rightarrow \pi^0 \nu \bar{\nu})$ and $\mathcal{B}(K^+ \rightarrow \pi^+ \nu \bar{\nu})$. The black dot represents the central value of the SM prediction.

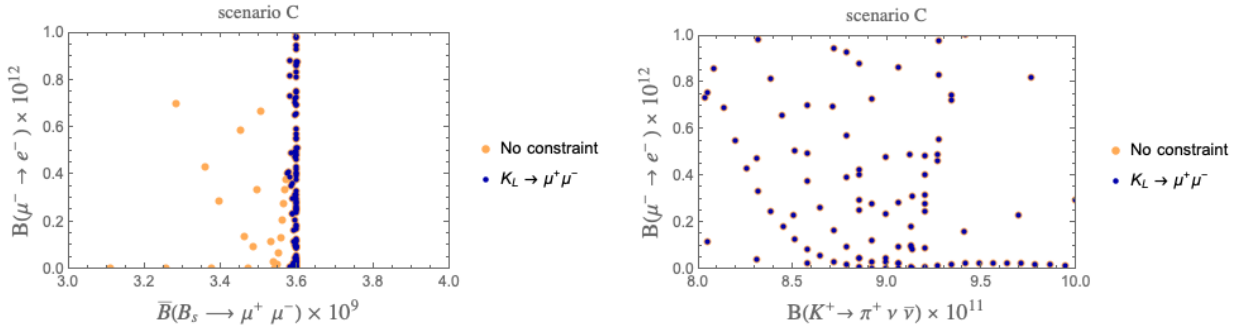


Figure 18: Scenario C. Correlations between $\mathcal{B}(\mu^- \rightarrow e^-)$ and $\bar{\mathcal{B}}(B_s \rightarrow \mu^+ \mu^-)$ (left panel) and between $\mathcal{B}(\mu^- \rightarrow e^-)$ and $\mathcal{B}(K^+ \rightarrow \pi^+ \nu \bar{\nu})$ (right panel).

7 Conclusions

We have presented a simple extension of the SM based on the introduction of a new U(1) gauge group. We have fulfilled the requirement of anomaly cancellation in a rather special way, defining the charges under the new group in terms of three new parameters

ϵ_i , $i = 1, 2, 3$ that are constrained to sum to zero, leaving only two as free parameters. Each of the three parameters governs one of the three fermion generations, so that quark and lepton sectors are connected to each other as far as their behaviour under the new gauge group is concerned. This leads to a constrained phenomenological panorama in which quark and lepton observables are correlated with each other. Independently of the structure of the Z' couplings to fermions, that we have varied considering a few scenarios, we have found that imposing bounds from experimental data relative to $\Delta F = 2$ processes to constrain quark flavour observables is not enough to prevent large deviations of these from their SM values. However, when constraints on lepton decays are imposed, the room for deviations is much reduced. In practice, quark and lepton sectors act simultaneously to produce a phenomenology similar to the SM. This can be a challenge to experiment but also shows that the pattern of data that we have at our disposal confirms the SM but does not exclude other scenarios like the one we are presenting.

We have also presented a scenario, following [57], in which a suitable hierarchy between LH and RH flavour violating couplings allows to remove the $\Delta F = 2$ constraints. In this case, as illustrated in a number of plots in Section 6.4, very large NP effects in all $\Delta F = 1$ observables can be obtained so that possible anomalies in various rare decays of mesons can easily be explained in the absence of pure leptonic decays. Yet as discussed on the examples of $K^+ \rightarrow \pi^+ \nu \bar{\nu}$ and $B_{s,d} \rightarrow \mu^+ \mu^-$ even in this case the imposition of the cancellation of gauge anomalies with the help of leptons has an important impact on the allowed values of their branching ratios. This is in particular the case of the experimental bound on $\mu - e$ conversion that eliminates any significant departures from the SM expectations of $B_{s,d} \rightarrow \mu^+ \mu^-$ and $K^+ \rightarrow \pi^+ \nu \bar{\nu}$ branching ratios as seen in Fig. 18.

The main lessons from our paper are the following ones:

- In models in which the gauge anomalies in the quark sector are cancelled by the corresponding anomalies in the lepton sector the impact of the present experimental bounds on leptonic processes, such as $\mu \rightarrow e \gamma$, $\mu \rightarrow e^- e^+ e^-$ and in particular $\mu - e$ conversion can be very large unless the model has more free parameters than the simple models considered by us.
- It appears then that a strategy for obtaining large NP effects while satisfying gauge anomaly cancellations is to construct models in which quark and lepton sectors are separately anomaly free.

Acknowledgements

We thank Robert Szafron for useful discussions. J.A. acknowledges financial support from the Swiss National Science Foundation (Project No. P400P2183838). The research of A.J.B and M. C-S was supported by the Excellence Cluster ORIGINS, funded by the Deutsche Forschungsgemeinschaft (DFG, German Research Foundation) under Germany's Excellence Strategy EXC-2094 390783311. The research of F.D.F. has been carried out within the INFN project (Iniziativa Specifica) QFT-HEP.

A Removing $\Delta F = 2$ Constraints

In the presence of both LH and RH couplings of a Z' gauge boson to SM quarks left-right (LR) $\Delta F = 2$ operators are generated whose contributions to the mixing amplitudes M_{12}^{bq} and M_{12}^{sd} in all three mesonic systems are enhanced through renormalisation group effects relative to left-left (VLL) and right-right (VRR) operators. Moreover in the case of M_{12}^{sd} additional chiral enhancements of the hadronic matrix elements of LR operators are present. As pointed out in [57] this fact can be used to suppress NP contributions to ε_K and ΔM_K through some fine-tuning between VLL, VRR and LR contributions, thereby allowing for larger contributions to $K \rightarrow \pi\pi$ amplitudes while satisfying the $\Delta S = 2$ constraints. In [58] this idea has been generalized to all three meson systems. While the fine-tuning required in the case of $K \rightarrow \pi\pi$ turned out to be rather large, it is more modest in case of $\Delta B = 2$ transitions.

We repeat here briefly the arguments presented in [57, 58]. Further details can be found in these two papers.

To this end we write the Z' contributions to the mixing amplitudes as follows [3]:

$$(M_{12}^*)_{Z'}^{sd} = \frac{(\Delta_L^{sd})^2}{2M_{Z'}^2} \langle \hat{Q}_1^{\text{VLL}}(M_{Z'}) \rangle^{sd} z_{sd}, \quad (102)$$

and

$$(M_{12}^*)_{Z'}^{bq} = \frac{(\Delta_L^{bq})^2}{2M_{Z'}^2} \langle \hat{Q}_1^{\text{VLL}}(M_{Z'}) \rangle^{bq} z_{bq}, \quad (103)$$

where z_{sd} and z_{bq} are generally complex. We have

$$z_{sd} = \left[1 + \left(\frac{\Delta_R^{sd}}{\Delta_L^{sd}} \right)^2 + 2\kappa_{sd} \frac{\Delta_R^{sd}}{\Delta_L^{sd}} \right], \quad \kappa_{sd} = \frac{\langle \hat{Q}_1^{\text{LR}}(M_{Z'}) \rangle^{sd}}{\langle \hat{Q}_1^{\text{VLL}}(M_{Z'}) \rangle^{sd}}, \quad (104)$$

with an analogous expressions for z_{bq} . Explicit expressions for the renormalisation scheme independent hadronic matrix elements and their values can be found in [58].

Now as seen in Table 5 of [58], both κ_{sd} and κ_{bq} are negative, implying that with the same sign of LH and RH couplings the last term in (104) could suppress the contribution of NP to $\Delta F = 2$ processes. One finds then that for $M_{Z'} \approx 5$ TeV one has $\kappa_{sd} \approx -115$ and $\kappa_{bq} \approx -4.3$ implying that for z_{sd} and z_{bq} to be significantly below unity the RH couplings must be much smaller than the LH ones. This in turn implies that the second quadratic term in the expression for z_{sd} in (104) can be neglected in first approximation, and we obtain the following hierarchy between LH and RH couplings necessary to suppress NP contributions to $\Delta F = 2$ observables:

$$\frac{\Delta_R^{sd}}{\Delta_L^{sd}} \simeq -\frac{a_{sd}}{2\kappa_{sd}}, \quad \frac{\Delta_R^{bq}}{\Delta_L^{bq}} \simeq -\frac{a_{bq}}{2\kappa_{bq}}. \quad (105)$$

The parameters a_{sd} and a_{bq} must be close to unity in order to make the suppression effective. How close they should be to unity depends on present and future results for hadronic and CKM parameters in $\Delta F = 2$ observables.

Unfortunately the present errors on the hadronic matrix elements are quite large, and do not allow a precise determination of the level of fine-tuning required. An estimate can be found in Fig. 6 of [58].

In any case the fact that a_{sd} and a_{bq} introduce in each case two new parameters allows us with some tuning of parameters to weaken the impact of $\Delta F = 2$ constraints on rare decays and even eliminate them which is not possible in LHS and RHS scenarios. On the other hand, due to the hierarchy of couplings and the absence of LR operators in the rare decays considered by us, rare decays are governed again by LH couplings as in the LHS, with the bonus that now the constraint from $\Delta F = 2$ observables can be ignored². As $\kappa_{sd} \gg \kappa_{bq}$ the hierarchy of couplings in this scenario must be much larger in the K system than in the $B_{s,d}$ systems.

The main message of [57, 58] is the following one: by appropriately choosing the hierarchy between LH and RH flavour violating Z' couplings to quarks one can eliminate to a large extent the constraints from $\Delta F = 2$ transitions even in the presence of large CP-violating phases at the price of sizable fine-tuning. But it should be noted that after the Z' has been integrated out, its LH and RH couplings are scale independent below $M_{Z'}$ and so for a given $M_{Z'}$ this tuning has to be done only once.

The implications of this are rather profound. Even if in the future the SM would agree perfectly with all $\Delta F = 2$ observables, this would not necessarily imply that no NP effects can be seen in rare decays. While, in particular in the K system, this requires some severe fine-tuning, we think it is interesting to consider this possibility.

References

- [1] P. Langacker, *The Physics of Heavy Z' Gauge Bosons*, *Rev. Mod. Phys.* **81** (2009) 1199–1228, [arXiv:0801.1345].
- [2] J. Erler, P. Langacker, S. Munir, and E. Rojas, *Improved Constraints on Z' -prime Bosons from Electroweak Precision Data*, *JHEP* **0908** (2009) 017, [arXiv:0906.2435].
- [3] A. J. Buras, F. De Fazio, and J. Girrbach, *The Anatomy of Z' and Z with Flavour Changing Neutral Currents in the Flavour Precision Era*, *JHEP* **1302** (2013) 116, [arXiv:1211.1896].
- [4] P. Langacker and M. Plumacher, *Flavor changing effects in theories with a heavy Z' boson with family nonuniversal couplings*, *Phys. Rev.* **D62** (2000) 013006, [hep-ph/0001204].
- [5] V. Barger, C.-W. Chiang, P. Langacker, and H.-S. Lee, *Z' mediated flavor changing neutral currents in B meson decays*, *Phys. Lett.* **B580** (2004) 186–196, [hep-ph/0310073].
- [6] V. Barger, C.-W. Chiang, J. Jiang, and P. Langacker, *$B_s - \bar{B}_s$ mixing in Z' models with flavor-changing neutral currents*, *Phys. Lett.* **B596** (2004) 229–239, [hep-ph/0405108].
- [7] V. Barger, L. L. Everett, J. Jiang, P. Langacker, T. Liu, et al., *$b \rightarrow s$ Transitions in Family-dependent $U(1)'$ Models*, *JHEP* **0912** (2009) 048, [arXiv:0906.3745].

²In the case of the correlation of $K_L \rightarrow \pi^0 \nu \bar{\nu}$ and $K^+ \rightarrow \pi^+ \nu \bar{\nu}$ this observation has been made first in [59], where the removal of the correlation of these decays with ε_K in the presence of both LH and RH couplings allowed to go beyond the two branch structure as seen by comparing the Figs. (3) and (7) in [58].

- [8] V. Barger, L. Everett, J. Jiang, P. Langacker, T. Liu, and C. Wagner, *Family Non-universal $U(1)$ -prime Gauge Symmetries and $b \rightarrow s$ Transitions*, *Phys. Rev. D* **80** (2009) 055008, [arXiv:0902.4507].
- [9] A. Celis, J. Fuentes-Martin, M. Jung, and H. Serodio, *Family nonuniversal Z' models with protected flavor-changing interactions*, *Phys. Rev. D* **92** (2015), no. 1 015007, [arXiv:1505.03079].
- [10] W. Altmannshofer, S. Gori, M. Pospelov, and I. Yavin, *Quark flavor transitions in $L_\mu - L_\tau$ models*, *Phys. Rev. D* **89** (2014) 095033, [arXiv:1403.1269].
- [11] M. Carena, A. Daleo, B. A. Dobrescu, and T. M. P. Tait, *Z' gauge bosons at the Tevatron*, *Phys. Rev. D* **70** (2004) 093009, [hep-ph/0408098].
- [12] J. Ellis, M. Fairbairn, and P. Tunney, *Anomaly-Free Dark Matter Models are not so Simple*, *JHEP* **08** (2017) 053, [arXiv:1704.03850].
- [13] G. D'Amico, M. Nardecchia, P. Panci, F. Sannino, A. Strumia, R. Torre, and A. Urbano, *Flavour anomalies after the R_{K^*} measurement*, *JHEP* **09** (2017) 010, [arXiv:1704.05438].
- [14] R. Alonso, P. Cox, C. Han, and T. T. Yanagida, *Anomaly-free local horizontal symmetry and anomaly-full rare B -decays*, *Phys. Rev. D* **96** (2017), no. 7 071701, [arXiv:1704.08158].
- [15] B. Allanach, F. S. Queiroz, A. Strumia, and S. Sun, *Z' models for the LHCb and $g - 2$ muon anomalies*, *Phys. Rev. D* **93** (2016), no. 5 055045, [arXiv:1511.07447]. [Erratum: *Phys. Rev. D* **95**, no. 11, 119902 (2017)].
- [16] F. Kahlhoefer, K. Schmidt-Hoberg, T. Schwetz, and S. Vogl, *Implications of unitarity and gauge invariance for simplified dark matter models*, *JHEP* **02** (2016) 016, [arXiv:1510.02110].
- [17] A. Ekstedt, R. Enberg, G. Ingelman, J. Löfgren, and T. Mandal, *Constraining minimal anomaly free $U(1)$ extensions of the Standard Model*, *JHEP* **11** (2016) 071, [arXiv:1605.04855].
- [18] A. Ismail, W.-Y. Keung, K.-H. Tsao, and J. Unwin, *Axial vector Z' and anomaly cancellation*, *Nucl. Phys. B* **918** (2017) 220–244, [arXiv:1609.02188].
- [19] J. Aebischer, C. Bobeth, and A. J. Buras, *On the Importance of NNLO QCD and Isospin-breaking Corrections in ϵ'/ϵ* , arXiv:1909.05610.
- [20] F. Feruglio, P. Paradisi, and A. Pattori, *On the Importance of Electroweak Corrections for B Anomalies*, *JHEP* **09** (2017) 061, [arXiv:1705.00929].
- [21] D. Buttazzo, A. Greljo, G. Isidori, and D. Marzocca, *B -physics anomalies: a guide to combined explanations*, *JHEP* **11** (2017) 044, [arXiv:1706.07808].
- [22] J. Aebischer, J. Kumar, P. Stangl, and D. M. Straub, *A Global Likelihood for Precision Constraints and Flavour Anomalies*, *Eur. Phys. J. C* **79** (2019), no. 6 509, [arXiv:1810.07698].
- [23] J. Aebischer, W. Altmannshofer, D. Guadagnoli, M. Reboud, P. Stangl, and D. M. Straub, *B -decay discrepancies after Moriond 2019*, arXiv:1903.10434.
- [24] N. Cabibbo, *Unitary Symmetry and Leptonic Decays*, *Phys. Rev. Lett.* **10** (1963) 531–533. [648(1963)].

- [25] M. Kobayashi and T. Maskawa, *CP Violation in the Renormalizable Theory of Weak Interaction*, *Prog. Theor. Phys.* **49** (1973) 652–657.
- [26] B. Pontecorvo, *Mesonium and antimesonium*, *Sov. Phys. JETP* **6** (1957) 429.
- [27] Z. Maki, M. Nakagawa, and S. Sakata, *Remarks on the unified model of elementary particles*, *Prog. Theor. Phys.* **28** (1962) 870.
- [28] J. Aebischer et al., *WCxf: an exchange format for Wilson coefficients beyond the Standard Model*, [arXiv:1712.05298](#).
- [29] J. Aebischer, A. Crivellin, M. Fael, and C. Greub, *Matching of gauge invariant dimension-six operators for $b \rightarrow s$ and $b \rightarrow c$ transitions*, *JHEP* **05** (2016) 037, [[arXiv:1512.02830](#)].
- [30] A. J. Buras, K. Gemmler, and G. Isidori, *Quark flavour mixing with right-handed currents: an effective theory approach*, *Nucl. Phys.* **B843** (2011) 107–142, [[arXiv:1007.1993](#)].
- [31] M. Blanke, A. J. Buras, K. Gemmler, and T. Heidsieck, *$\Delta F = 2$ observables and $B \rightarrow X_q \gamma$ in the Left-Right Asymmetric Model: Higgs particles striking back*, *JHEP* **1203** (2012) 024, [[arXiv:1111.5014](#)].
- [32] I. Esteban, M. C. Gonzalez-Garcia, A. Hernandez-Cabezudo, M. Maltoni, and T. Schwetz, *Global analysis of three-flavour neutrino oscillations: synergies and tensions in the determination of θ_{23} , δ_{CP} , and the mass ordering*, *JHEP* **01** (2019) 106, [[arXiv:1811.05487](#)].
- [33] A. J. Buras, F. De Fazio, J. Girrbach, and M. V. Carlucci, *The Anatomy of Quark Flavour Observables in 331 Models in the Flavour Precision Era*, *JHEP* **1302** (2013) 023, [[arXiv:1211.1237](#)].
- [34] A. J. Buras, *New physics patterns in ϵ'/ϵ and ϵ_K with implications for rare kaon decays and ΔM_K* , *JHEP* **04** (2016) 071, [[arXiv:1601.00005](#)].
- [35] J. Aebischer, C. Bobeth, A. J. Buras, and D. M. Straub, *Anatomy of ϵ'/ϵ beyond the standard model*, *Eur. Phys. J.* **C79** (2019), no. 3 219, [[arXiv:1808.00466](#)].
- [36] J. Aebischer, C. Bobeth, A. J. Buras, J.-M. Gérard, and D. M. Straub, *Master formula for ϵ'/ϵ beyond the Standard Model*, *Phys. Lett.* **B792** (2019) 465–469, [[arXiv:1807.02520](#)].
- [37] J. Aebischer, A. J. Buras, and J.-M. Gérard, *BSM hadronic matrix elements for ϵ'/ϵ and $K \rightarrow \pi\pi$ decays in the Dual QCD approach*, *JHEP* **02** (2019) 021, [[arXiv:1807.01709](#)].
- [38] J. Aebischer, M. Fael, C. Greub, and J. Virto, *B physics Beyond the Standard Model at One Loop: Complete Renormalization Group Evolution below the Electroweak Scale*, *JHEP* **09** (2017) 158, [[arXiv:1704.06639](#)].
- [39] E. E. Jenkins, A. V. Manohar, and P. Stoffer, *Low-Energy Effective Field Theory below the Electroweak Scale: Anomalous Dimensions*, *JHEP* **01** (2018) 084, [[arXiv:1711.05270](#)].
- [40] M. Lindner, M. Platscher, and F. S. Queiroz, *A Call for New Physics : The Muon Anomalous Magnetic Moment and Lepton Flavor Violation*, *Phys. Rept.* **731** (2018) 1–82, [[arXiv:1610.06587](#)].

- [41] **MEG** Collaboration, A. M. Baldini et al., *Search for the lepton flavour violating decay $\mu^+ \rightarrow e^+\gamma$ with the full dataset of the MEG experiment*, *Eur. Phys. J.* **C76** (2016), no. 8 434, [[arXiv:1605.05081](#)].
- [42] **BaBar** Collaboration, B. Aubert et al., *Searches for Lepton Flavor Violation in the Decays $\tau^\pm \rightarrow e^\pm\gamma$ and $\tau^\pm \rightarrow \mu^\pm\gamma$* , *Phys. Rev. Lett.* **104** (2010) 021802, [[arXiv:0908.2381](#)].
- [43] D. M. Straub, *flavio: a Python package for flavour and precision phenomenology in the Standard Model and beyond*, [arXiv:1810.08132](#).
- [44] A. Brignole and A. Rossi, *Anatomy and phenomenology of $\mu\tau$ lepton flavour violation in the MSSM*, *Nucl. Phys.* **B701** (2004) 3–53, [[hep-ph/0404211](#)].
- [45] A. Crivellin, S. Najjari, and J. Rosiek, *Lepton Flavor Violation in the Standard Model with general Dimension-Six Operators*, *JHEP* **04** (2014) 167, [[arXiv:1312.0634](#)].
- [46] **HFLAV** Collaboration, Y. S. Amhis et al., *Averages of b -hadron, c -hadron, and τ -lepton properties as of 2018*, [arXiv:1909.12524](#). updated results and plots available at <https://hflav.web.cern.ch/>.
- [47] **Particle Data Group** Collaboration, M. Tanabashi et al., *Review of Particle Physics*, *Phys. Rev.* **D98** (2018), no. 3 030001.
- [48] J. Hisano, T. Moroi, K. Tobe, and M. Yamaguchi, *Lepton-Flavor Violation via Right-Handed Neutrino Yukawa Couplings in Supersymmetric Standard Model*, *Phys. Rev.* **D53** (1996) 2442–2459, [[hep-ph/9510309](#)].
- [49] J. Bernabeu, E. Nardi, and D. Tommasini, *$\mu - e$ conversion in nuclei and Z' physics*, *Nucl. Phys.* **B409** (1993) 69–86, [[hep-ph/9306251](#)].
- [50] T. Suzuki, D. F. Measday, and J. P. Roalsvig, *Total nuclear capture rates for negative muons*, *Phys. Rev. C* **35** (Jun, 1987) 2212–2224.
- [51] **SINDRUM II** Collaboration, W. H. Bertl et al., *A Search for muon to electron conversion in muonic gold*, *Eur. Phys. J.* **C47** (2006) 337–346.
- [52] G. Isidori and R. Unterdorfer, *On the short distance constraints from $K_{(L,S)} \rightarrow \mu^+\mu^-$* , *JHEP* **01** (2004) 009, [[hep-ph/0311084](#)].
- [53] **CMS** Collaboration, S. Chatrchyan et al., *Measurement of the $B_s \rightarrow \mu\mu$ branching fraction and search for $B_0 \rightarrow \mu\mu$ with the CMS Experiment*, *Phys. Rev. Lett.* **111** (2013) 101804, [[arXiv:1307.5025](#)].
- [54] **LHCb, CMS** Collaboration, V. Khachatryan et al., *Observation of the rare $B_s^0 \rightarrow \mu^+\mu^-$ decay from the combined analysis of CMS and LHCb data*, *Nature* **522** (2015) 68–72, [[arXiv:1411.4413](#)].
- [55] **LHCb** Collaboration, R. Aaij et al., *Measurement of the $B_s^0 \rightarrow \mu^+\mu^-$ branching fraction and effective lifetime and search for $B^0 \rightarrow \mu^+\mu^-$ decays*, *Phys. Rev. Lett.* **118** (2017), no. 19 191801, [[arXiv:1703.05747](#)].
- [56] **ATLAS** Collaboration, M. Aaboud et al., *Study of the rare decays of B_s^0 and B^0 mesons into muon pairs using data collected during 2015 and 2016 with the ATLAS detector*, *JHEP* **04** (2019) 098, [[arXiv:1812.03017](#)].
- [57] A. J. Buras, F. De Fazio, and J. Girrbach, *$\Delta I = 1/2$ rule, ε'/ε and $K \rightarrow \pi\nu\bar{\nu}$ in $Z'(Z)$ and G' models with FCNC quark couplings*, *Eur. Phys. J.* **C74** (2014) 2950, [[arXiv:1404.3824](#)].

-
- [58] A. J. Buras, D. Buttazzo, J. Girrbach-Noe, and R. Knegjens, *Can we reach the Zeptouniverse with rare K and $B_{s,d}$ decays?*, *JHEP* **1411** (2014) 121, [[arXiv:1408.0728](#)].
- [59] M. Blanke, *Insights from the Interplay of $K \rightarrow \pi\nu\bar{\nu}$ and ϵ_K on the New Physics Flavour Structure*, *Acta Phys.Polon.* **B41** (2010) 127, [[arXiv:0904.2528](#)].